Supporting Information

A copper-seamed metal-organic capsule as a semiconductor photocatalyst for molecular oxygen activation

Xiangquan Hu, Meirong Han, Leicheng Wang, Li Shao, Peeyush, Yadav, Jialei Du*, Steven P. Kelley, Scott J. Dalgarno, David A. Atwood, Sisi Feng*, and Jerry L. Atwood*

Supplementary Methods

Materials and Characterization. All solvents and chemicals were purchased from commercial sources and used without further purification.

Single-crystal X-ray diffraction (SCXRD) data were measured on a Bruker SMART diffractometer equipped with an Apex II CCD area detector (Bruker AXS, Madison, WI, USA) and a Mo-Kα X-ray source with focusing optics (λ = 0.70174 Å). A single crystal was isolated under an optical polarizing microscope, mounted on a polyimide loop using heavy hydrocarbon oil, and cooled to the collection temperature under a stream of cold N_2 gas using an Oxford Cryostream 700 cryostat (Oxford Cryosystems, Oxford, UK). A hemisphere of unique data was collected out to a resolution of 0.80 Å using strategies of scans about the omega and phi axes. The resolution of the data was truncated to 1.0 Å during integration; the average signal-to-noise ratio of the data from the 1.02-1.00 Å shell is 0.47, indicating the data beyond this resolution is indistinguishable from noise. Data collection, unit cell determination, data reduction, absorption correction and scaling, and space group determination were done using the Bruker Apex3 software suite.[1]

The crystal structure was solved by an iterative dual-space method as implemented in SHELXT,[2] and refined by full matrix least squares refinement against $|F^2|$ using SHELXL v. 2017.[3] The metal atoms, phenyl group carbon and oxygen atoms, and atoms corresponding to ordered DMF and pyridine ligands could all be refined anisotropically. Five large difference map peaks were located inside the capsule at positions roughly equidistant from two Cu ions with Cu-X-Cu angles close to 90°. These peaks could not be modeled as oxygen atoms without refining to negative isotropic displacement parameters, but they were not large enough to be modeled as full-occupancy bromide ions. These five positions were modeled as bromine atoms at 30% occupancy, which corresponds to 3 bromide ions per capsule, and could be refined anisotropically. The positions suggest that the ions are randomly disordered across endohedral, axial coordination sites for the Cu ions. Restraints for rigid bond behavior were applied to all anisotropic thermal displacement parameters in order to compensate for the large number of parameters caused by the complexity of its structure, its disorder, and the absence of strong high-angle diffraction.[4]

Six of the pentyl chains were disordered, and the multiple overlapping conformations could not be resolved and refined even with the aid of restraints. The most strongly affected carbon atoms were refined isotropically, and the atomic displacement parameters are interpreted as defining the volume across which the alkyl chains are disordered. Four of these chains could not be modeled with any

chemically reasonable connectivity for a pentyl group, so all difference map peaks in the region were assigned as carbon atoms, and if more than five peaks were present the occupancies of all atoms were fixed to fractions so that the total number of carbon atoms summed to 5. For two of these chains, it was not possible to locate five peaks from the difference map, so the missing carbon atoms are excluded from the model. The inability to locate some of the most severely disordered carbon atoms is probably caused by the low resolution of the data set, along with the large number of refined parameters associated with the ordered part of the structure. Examination of the packing reveals that the well-ordered pentyl groups are associated with capsules that interface vertex-to-vertex, which allows the pentyl groups to interdigitate. The disordered pentyl groups are associated with PgC_5 groups that are oriented such that the pentyl groups are aimed at capsule faces and engage in repulsive interactions with axial ligands and other pentyl groups.

An axial, exocyclic ligand bonded to Cu1 was modeled as a pyridine ligand using geometric restraints to keep the atoms planar and the bond distances similar in magnitude. This group was refined isotropically with unusually large thermal parameters for the carbon atoms. A DMF ligand disordered by 180° rotation about the Cu-O bond axis would also be consistent with the difference map peaks, so the identity of this ligand is uncertain.

The model, including all disorder described above, contains 3150 $Å^3$ of solvent-accessible void volume per unit cell, and the difference map could not be modeled in any meaningful way. The contribution of disordered solvent in this region was estimated and excluded from |Fobs| using a solvent mask routine as implemented in PLATON SQUEEZE. The analysis found 750 e^-/unit cell of disordered matter.

Powder XRD data was collected on a Bruker Apex II CCD diffractometer using Cu (Kα) radiation Inco-tech Microfocus II (1.5406 Å). In order to avoid changes in the crystal structure due to desolvation, samples were pulverized by hand with a steel spatula tip while covered with the mother liquor, and the resulting slurry was loaded into a 0.5 mm flexible polyimide capillary. The loaded capillary was aligned on the diffractometer so that a slug of powder was centered in the X-ray beam. Data was collected across a 2θ range of 3 to 40°. The area detector was centered at 20° at a sample-to-detector distance of 8.00 cm, and eight consecutive 60s long exposures were collected while rotating the sample 360° about the phi axis for each exposure. The area detector photographs were reduced using the Apex3 software suite by integrating a 64°-wide sector of the frame in radial shells with widths of 0.02°.

Nuclear magnetic resonance spectra (NMR) spectra were recorded on Bruker AV-400/600 (400/600 MHz) spectrometers. Chemical shifts (in ppm) were referenced to tetramethylsilane (δ = 0 ppm) in $CDCl_3$ as an internal standard. Data for ^1H NMR are reported as follows: chemical shifts (δ ppm), multiplicity (s = singlet, brs = broad singlet, d = doublet, t = triplet, dd = doublet of doublets, dt = doublet of triplets, m = multiplet), coupling constant (Hz) and integration.

The FT-IR spectra were recorded on a Bruker Tensor 27 spectrometer with KBr disks.

MALDI (Matrix-Assisted Laser Desorption Ionization) TOF (Time of Flight) mass spectrometer (MS) was measured on a MALDI TOF MS Bruker Flex Speed MALID Mass spectrometer. Samples were dissolved in dichloromethane (DCM) and mixed with MALDI matrix dithranol solution (10 mg/mL in DCM).

Elemental analysis (EA) was performed using a Vario EL III analyzer.

UV-vis diffuse reflectance (DRS) spectra were performed using a TU-1950 UV-vis spectrophotometer, during which $BaSO_4$ was adopted as the internal reflectivity standard.

Electron paramagnetic resonance (ESR) trapping experiments. For the detection of $O_2^{\bullet-}$, 40 μL of DMPO was mixed with 0.5 mL MONC-MeOH suspension (4 mg/mL). From the obtained mixture, 400 μL was taken and added into the EPR tube. The ESR tube was tested in the dark or under light irradiation (300 W Xe lamp with 420 nm cutoff). For the detection of $^1O_2$, similar procedures were adopted except the use of TEMP as the spin-trapping agent. For the detection of •OH, 40 μL of DMPO was mixed with 0.5 mL of aqueous suspension of samples (4 mg/mL).

Photocurrent measurements were conducted with a CHI 660E electrochemical workstation in a standard three-electrode system with a working electrode, a platinum plate as the counter electrode, and an Hg/Hg_2Cl_2 (SCE) as a reference electrode. 0.1 M Na_2SO_4 aqueous solution (pH=7.0) was chosen as the supporting electrolyte. A 300 W xenon lamp with a UV cutoff filter (λ> 420 nm) was used as the light source. The light intensity was adjusted to 100 mW/cm^2 using an optical power meter (CEL-NP2000, CEAULIGHT, Beijing). The photocurrent signals were recorded under chopped light illumination with an interval 60 s.

General procedure for photocatalytic oxidative hydroxylation of boronic acids. Boronic acids (0.4 mmol), catalyst (10 mg), triethylamine (0.8 mmol, 2.0 equiv.), and H_2O (3.0 mL) were added to a 10 mL glass tube with a stir bar. Prior to the reaction, the tube was filled with oxygen. The mixture was stirred vigorously and irradiated with a 300 W xenon lamp equipped with an UV cutoff filter (λ> 420 nm) at a fixed light intensity of 100 mW/cm^2. The reaction process was monitored by thin-layer chromatography (TLC). After completion, reaction mixture was filtered to separate the solid catalyst. The solid catalyst was washed with methanol several times and dried in vacuum for next cycle practice. The collected filtrate was extracted with ethyl acetate (3 × 10 mL). The combined organic layer was dried over anhydrous sodium sulphate and concentrated under reduced pressure. The crude product was purified by column chromatography (silica gel) to give the target product, using petroleum ether (PE) /ethyl acetate (EA) as the eluent.

Procedure for photocatalytic oxidative dehydrogenation of 1,2-diphenylhydrazine. 1,2-diphenylhydrazine (0.1 mmol), catalyst (10 mg), MeOH (2 mL), and H_2O (0.5 mL) were added to a 10 mL glass tube with a stir bar. Prior to the reaction, the tube was filled with oxygen. The mixture was stirred vigorously and irradiated with a 300 W xenon lamp equipped with an UV cutoff filter (λ> 420 nm) at a fixed light intensity of 100 mW/cm^2. The reaction process was monitored by thin-layer chromatography (TLC). After completion, reaction mixture was filtered to separate the solid catalyst. The solid catalyst was washed with methanol several times and dried in vacuum for next cycle practice. The collected filtrate was concentrated under reduced pressure. The target product was obtained without purification.

Procedure for photocatalytic oxidative coupling of benzylamine. benzylamine (0.2 mmol), catalyst (10 mg), and MeOH (2.0 mL) were added to a 10 mL glass tube with a stir bar. Prior to the reaction, the tube was filled with oxygen. The mixture was stirred vigorously and irradiated with a 300 W xenon lamp equipped with an UV cutoff filter (λ> 420 nm) at a fixed light intensity of 100 mW/cm^2. The reaction process was monitored by thin-layer chromatography (TLC). After completion, reaction mixture was filtered to separate the solid catalyst. The solid catalyst was washed with methanol several times and dried in vacuum for next cycle practice. The collected filtrate was concentrated under reduced pressure. The target product was obtained without purification.

Synthesis of C-pentyl-pyrogallol[4]arene (PgC_5). Hexanal (10 ml, 0.08 mol) and pyrogallol (10.0 g, 0.08 mol) were mixed in 30 mL of ethanol and then 3.5 mL of concentrated HCl was added as a catalyst. The mixture was refluxed at 100 °C for 24 hours and cooled to room temperature. The resultant crystalline precipitate was filtered, washed with cold ethanol/water (1:1) and dried under vacuum. Yield is 35.5%.[5]

Synthesis of 1. PgC_5 (83.2 mg, 0.1 mmol) and cuprous bromide (0.4 mmol, 57.4 mg) were added to a mixed solvent of DMF (2 mL), methanol (3 mL) and pyridine (200 µL, 1.2 mmol). The mixture was sealed in 8 mL glass vial, which was heated at 100 °C for 3 h to afford clear red solution. After slow concentration of the filtrate at room temperature for 48 hours, dark red single crystals of **1** were obtained (yield: 74 mg, 56.1% based on the PgC_5 ligand), which were washed with methanol and water. Unit cells of several crystals from different vials were checked in order to establish sample homogeneity. Elemental analysis (%): observed C 50.34, H 5.75, N 1.80, calculated for $C_{333}H_{453}O_{97}N_{10}Br_3Cu_{24}$, $[Cu_{24}(PgC_5)_6(Br)_3(H_2O)_{12}(C_5H_5N)_4(C_3H_7NO)_4(CH_3OH)_7]\cdot(DMF)_2$, C 50.54, H 5.77, N 1.77.

Crystallographic information for **1**: brown irregular, 0.42 x 0.2 x 0.05 mm^3, triclinic, space group *P*-1 (No. 2), a = 22.579(8), b = 22.754(8), c = 24.113(8) Å, α = 108.799(5)°, β = 106.390(5)°, γ = 104.441(5)°, V = 10431(6) $Å^3$, Z = 1, Dc = 1.224 g cm^{-3}, F_{000} = 3972, Bruker APEX II area detector, MoKα radiation, λ = 0.71073 Å, T = 150.0 K, $2\theta_{max}$ = 42.2°, 82759 reflections collected, 22443 unique (R_{int} = 0.1828). Final GooF = 1.132, R_1 = 0.1196, wR_2 = 0.3193, R indices based on 10052 reflections with I> 2σ(I) (refinement on F^2), 1896 parameters, 1892 restraints. Lp and absorption corrections applied, µ = 1.548 mm^{-1}.

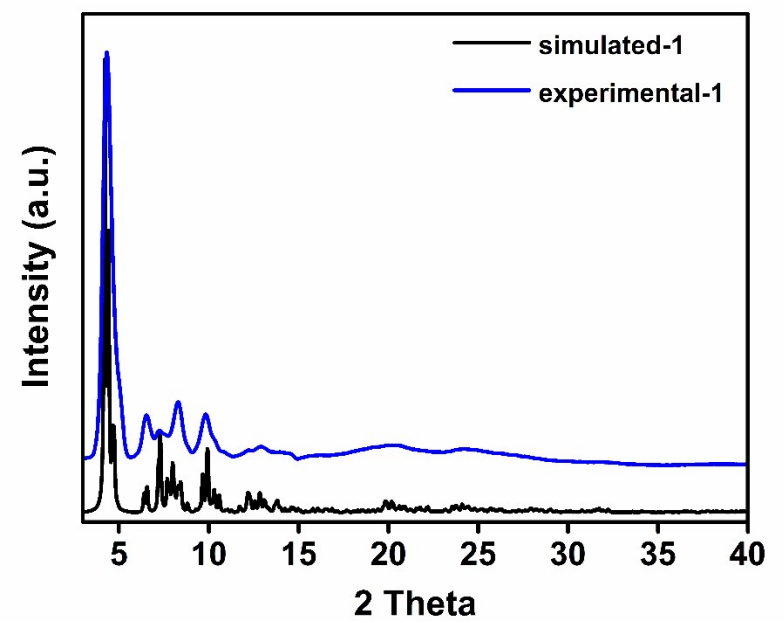

Figure. S1. Simulated and experimental X-ray diffraction powder pattern of **1**.

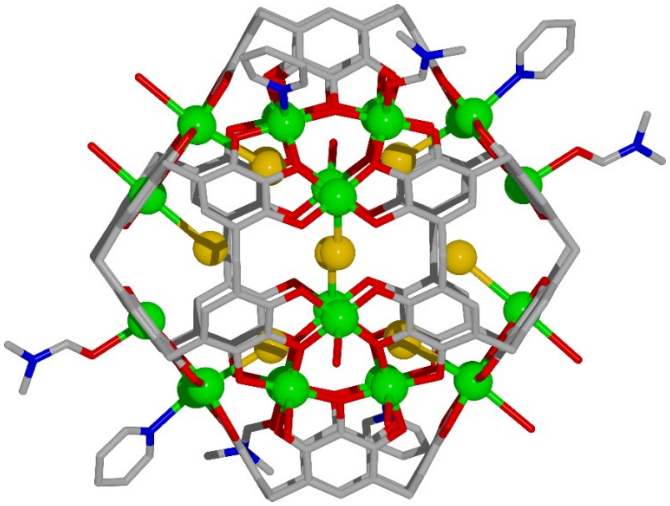

Figure. S2. Side view of **1**. Hydrogen atoms and alkyl tails have been omitted for clarity. Color codes: C, gray; O, red; Br, orange; Cu, green.

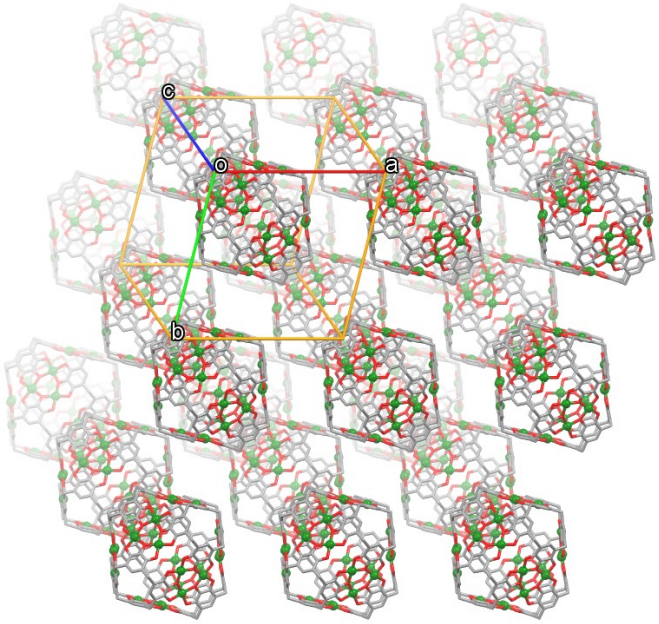

Figure. S3. Extended view of **1**. Hydrogen atoms, alkyl tails, and axial ligands have been omitted for clarity. Color codes: C, gray; O, red; Cu, green.

Table S1. Bond-valence sum (BVS) analysis for **1**.[6]

Identity	Calculated Value		Assignment
	Cu^{+}	Cu^{2+}	
Cu1	1.733367	2.231112	+2
Cu2	1.693675	2.148432	+2
Cu3	1.734182	2.228678	+2
Cu4	1.736886	2.229125	+2
Cu5	1.623915	2.059942	+2
Cu6	1.575346	1.998331	+2
Cu7	1.490899	1.89121	+2
Cu8	1.508285	1.913265	+2
Cu9	1.578325	2.002111	+2
Cu10	1.588477	2.014989	+2
Cu11	1.615617	2.072518	+2
Cu12	1.534755	1.946843	+2

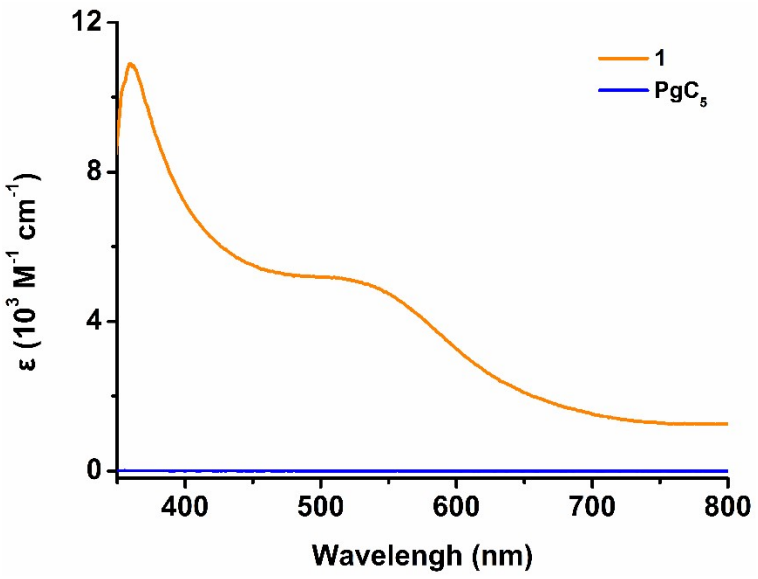

Figure S4. UV–vis absorption spectra of **1** (orange line) and **PgC_5** (blue line) in chloroform.

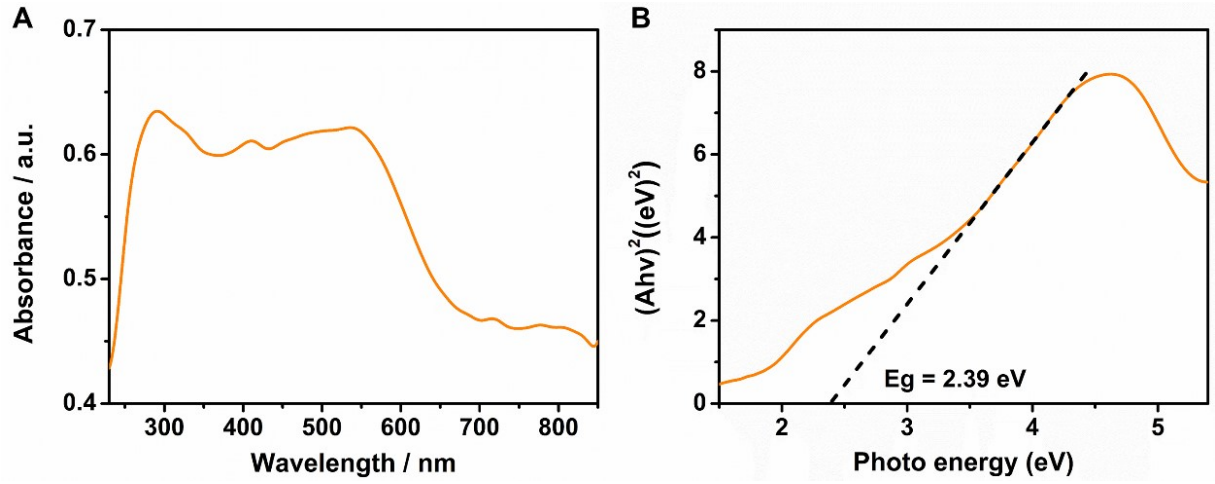

Figure S5. UV-Vis diffuse reflectance spectrum (a) and Tauc plot (b) of **1.**

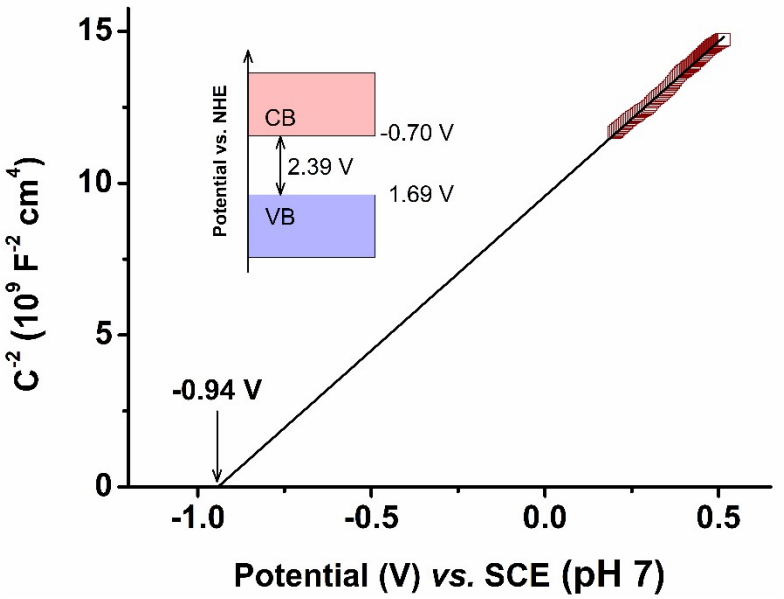

Figure S6. Mott-Schottky plots of **1** in 0.1 M Na_2SO_4 aqueous solution. Inset: the electronic band structures of **1**.

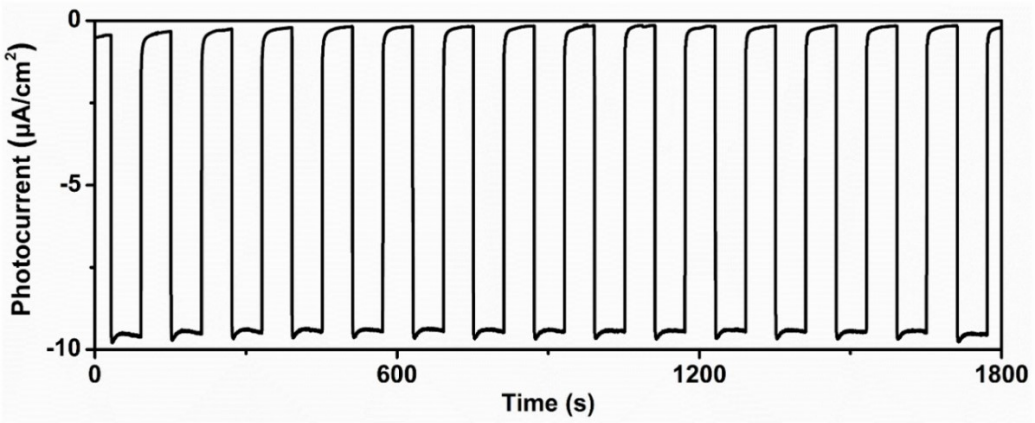

Figure S7. Transient photocurrent response of **1** in 0.1 M air-saturated Na_2SO_4 aqueous solution under visible-light irradiation (λ> 420 nm) at 0 V vs. SCE.

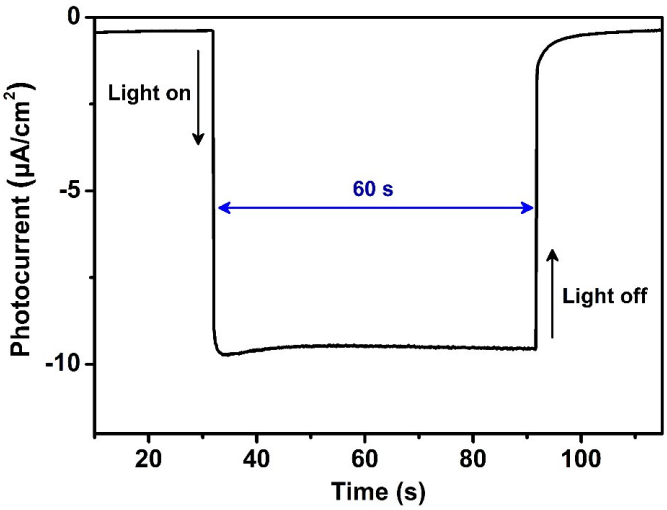

Figure S8. Transient photocurrent response of **1** in 0.1 M air-saturated Na_2SO_4 aqueous solution under visible-light irradiation (λ> 420 nm) at 0 V vs. SCE.

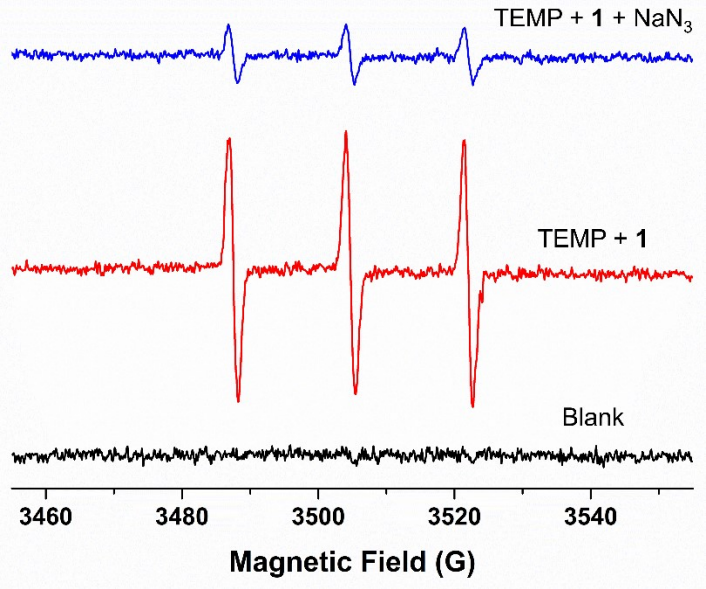

Figure S9. ESR spectra of **1** in the presence of TEMP and NaN_3 under light conditions in methanol.

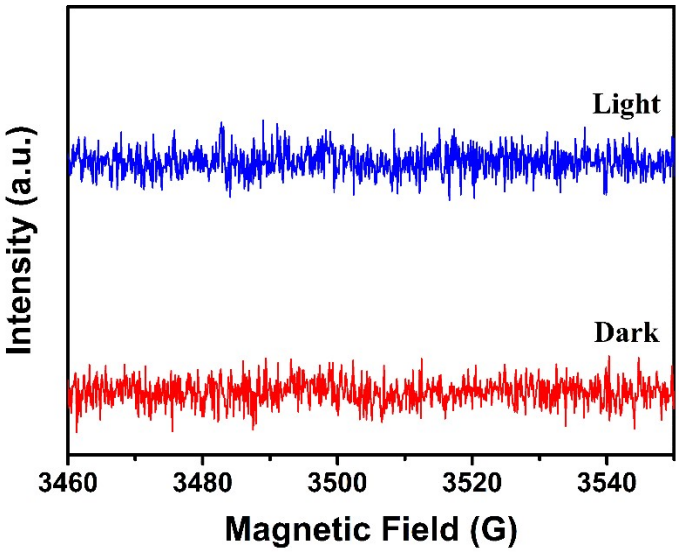

Figure S10. ESR spectra of **1** in the presence of DMPO under dark and light conditions in water.

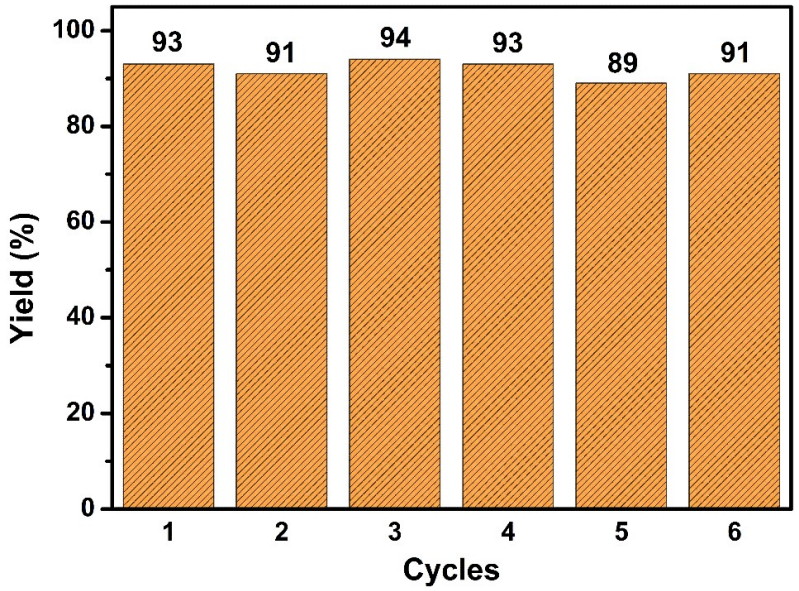

Figure S11. Recycling performance of **1** in photocatalytic oxidative hydroxylation of phenylboronic acid.

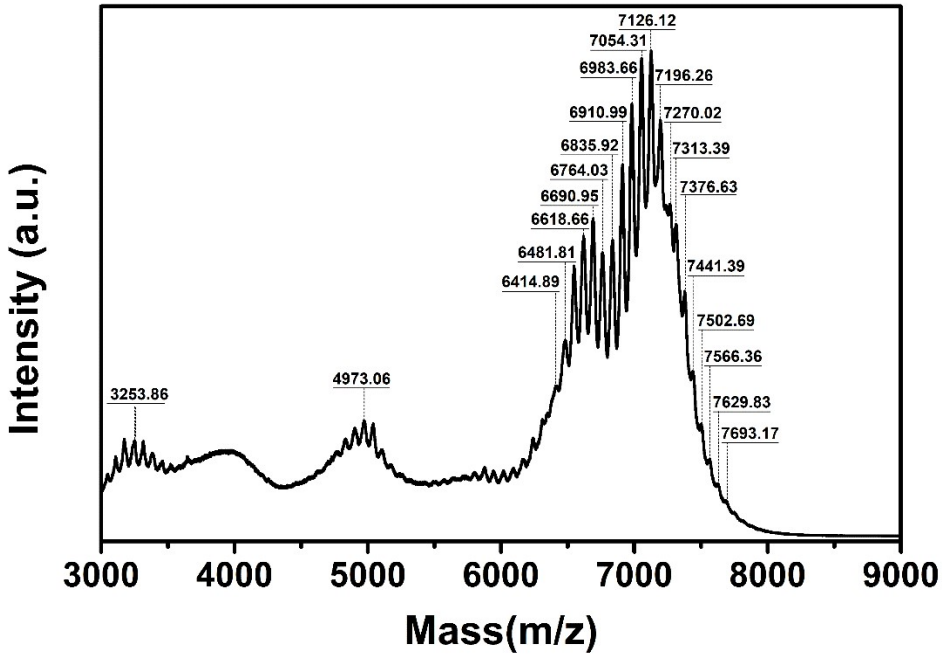

Figure S12. MALDI-TOF MS spectrum of **1**.

Table S2. Structural assignment of partial peaks in MALDI-TOF spectrum of **1**.

Found m/z (Da)	Calculated m/z (Da)	[Fragment]$^+$	Formula
7693.17	7693.79	$[Cu_{24}(PgC_5)_6(Br)_3(H_2O)_{12}(C_5H_5N)_4(CH_3OH)_7(C_3H_7NO)_3]^+$	$C_{324}H_{432}O_{94}N_7Br_3Cu_{24}$
7629.83	7629.71	$[Cu_{24}(PgC_5)_6(Br)_3(H_2O)_{12}(C_5H_5N)_4(CH_3OH)_5(C_3H_7NO)_3]^+$	$C_{322}H_{424}O_{92}N_7Br_3Cu_{24}$
7566.36	7566.65	$[Cu_{24}(PgC_5)_6(Br)_3(H_2O)_9(C_5H_5N)_4(CH_3OH)_7(C_3H_7NO)_2]^+$	$C_{321}H_{419}O_{90}N_6Br_3Cu_{24}$
7502.69	7502.57	$[Cu_{24}(PgC_5)_6(Br)_3(H_2O)_9(C_5H_5N)_4(CH_3OH)_5(C_3H_7NO)_2]^+$	$C_{319}H_{411}O_{88}N_6Br_3Cu_{24}$
7441.39	7441.48	$[Cu_{24}(PgC_5)_6(Br)_3(H_2O)_{10}(C_5H_5N)_3(CH_3OH)_5(C_3H_7NO)_2]^+$	$C_{314}H_{408}O_{89}N_5Br_3Cu_{24}$
7376.63	7376.46	$[Cu_{24}(PgC_5)_6(Br)_3(H_2O)_2(C_5H_5N)_4(CH_3OH)_5(C_3H_7NO)_2]^+$	$C_{319}H_{397}O_{81}N_6Br_3Cu_{24}$
7313.39	7313.36	$[Cu_{24}(PgC_5)_6(Br)_3(H_2O)_5(C_5H_5N)_2(CH_3OH)_4(C_3H_7NO)_3]^+$	$C_{311}H_{396}O_{84}N_5Br_3Cu_{24}$
7270.02	7270.28	$[Cu_{24}(PgC_5)_6(Br)_3(H_2O)_7(C_5H_5N)(CH_3OH)_4(C_3H_7NO)_3]^+$	$C_{306}H_{395}O_{86}N_4Br_3Cu_{24}$
7196.26	7196.21	$[Cu_{24}(PgC_5)_6(Br)_3(H_2O)_4(C_5H_5N)_3(CH_3OH)_3(C_3H_7NO)]^+$	$C_{309}H_{381}O_{80}N_4Br_3Cu_{24}$
7126.12	7126.11	$[Cu_{24}(PgC_5)_6(Br)_3(H_2O)_4(C_5H_5N)_3(CH_3OH)_5]^+$	$C_{303}H_{379}O_{82}N_2Br_3Cu_{24}$
7054.31	7054.05	$[Cu_{24}(PgC_5)_6(Br)_3(H_2O)(C_5H_5N)_2(CH_3OH)_5]^+$	$C_{303}H_{371}O_{78}N_2Br_3Cu_{24}$
6983.66	6983.96	$[Cu_{24}(PgC_5)_6(Br)_3(H_2O)(C_5H_5N)(CH3OH)_3(C_3H_7NO)]^+$	$C_{299}H_{365}O_{77}N_2Br_3Cu_{24}$
6910.99	6910.87	$[Cu_{24}(PgC_5)_6(Br)_3(H_2O)(C_5H_5N)(CH3OH)_3]^+$	$C_{296}H_{358}O_{76}NBr_3Cu_{24}$
6835.92	6835.75	$[Cu_{24}(PgC_5)_6(Br)_3(H_2O)_3(CH_3OH)_2]^+$	$C_{290}H_{353}O_{77}Br_3Cu_{24}$
6764.03	6764.86	$[Cu_{24}(PgC_5)_6(Br)_2(H_2O)_3(C_3H_7NO)]^+$	$C_{291}H_{352}O_{76}NBr_2Cu_{24}$

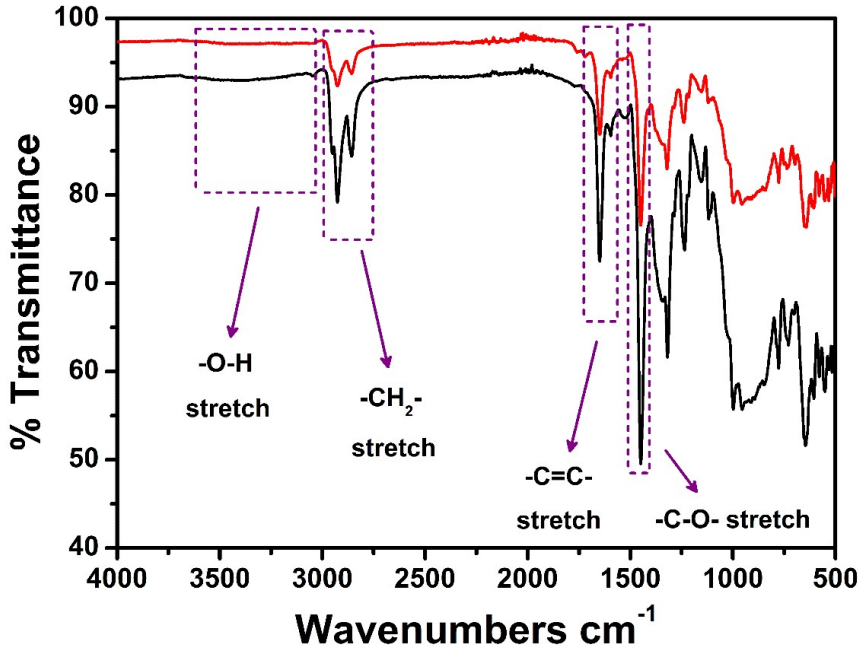

Figure S13. IR spectra of **1** (black line) and recycled **1** (red line).

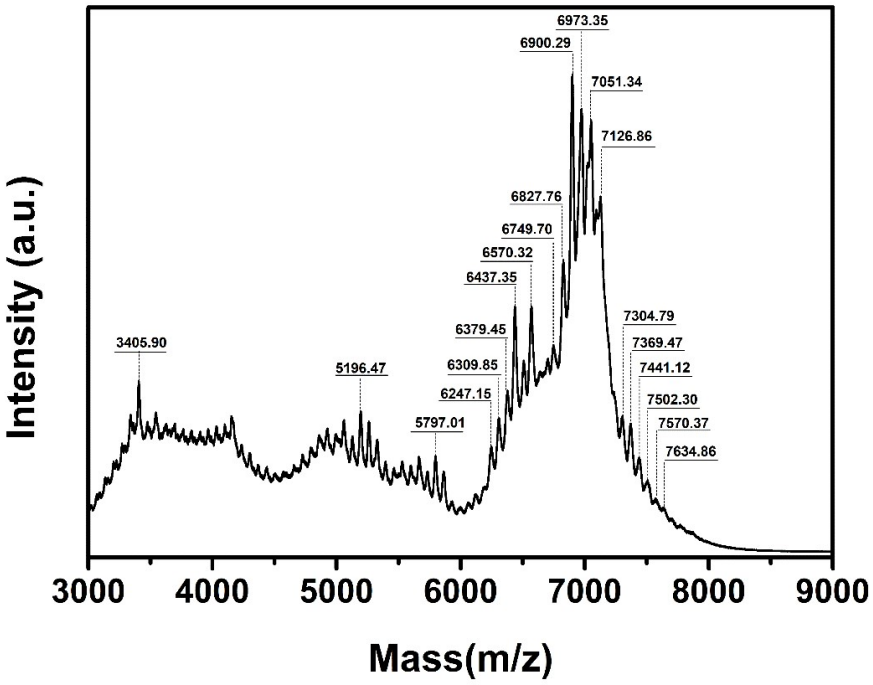

Figure S14. MALDI-TOF MS spectrum of recycled **1**.

Table S3. Photocatalytic oxidative hydroxylation of boronic acids.[a]

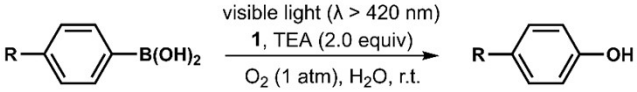

entry	substrate	product	time (h)	yield (%)[b]
1	R= H	R = H	5	93
2	R= Me	R = Me	5	90
3	R= OMe	R= OMe	6	89
4	R= Cl	R = Cl	5	91
5	R= CN	R= CN	5	93
6	R= CHO	R= CHO	5	88
7	R= COOH	R = COOH	5	92
8	R= Ph	R= Ph	5	89
9	R =OH	R= OH	6	84
10	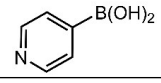	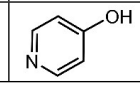	6	88

[a]Reaction condition: **1** (10 mg), boronic acids (0.4 mmol), O_2 (1 atm), 3 mL water, 300 W xenon lamp with visible light (λ > 420 nm, 100 mW/cm^2), room temperature. [b]Isolated yield.

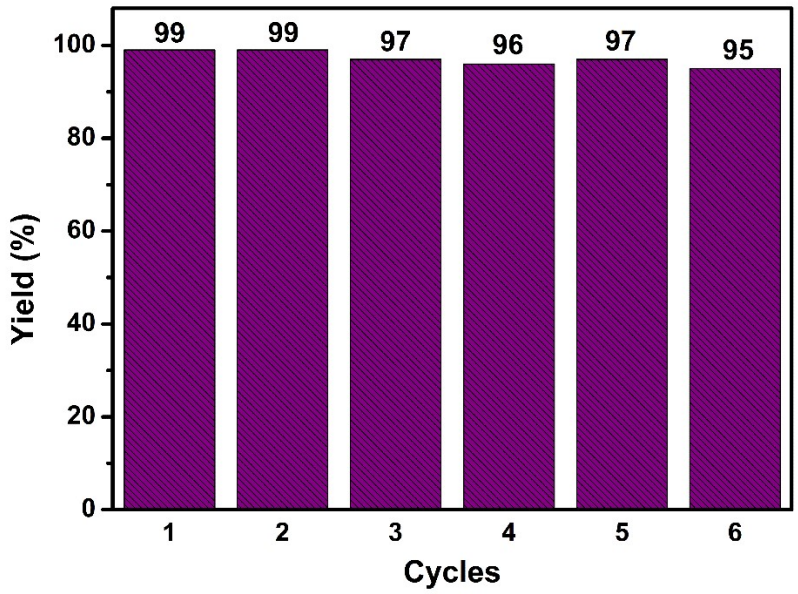

Figure S15. Recycling performance of **1** in photocatalytic oxidative dehydrogenation of 1,2-diphenylhydrazine.

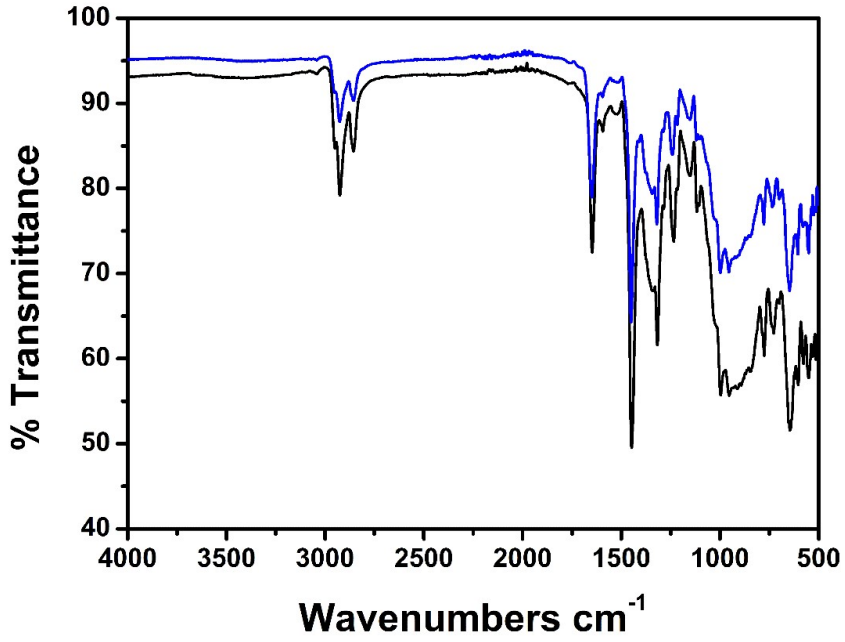

Figure S16. IR spectra of **1** (black line) and recycled **1** (blue line).

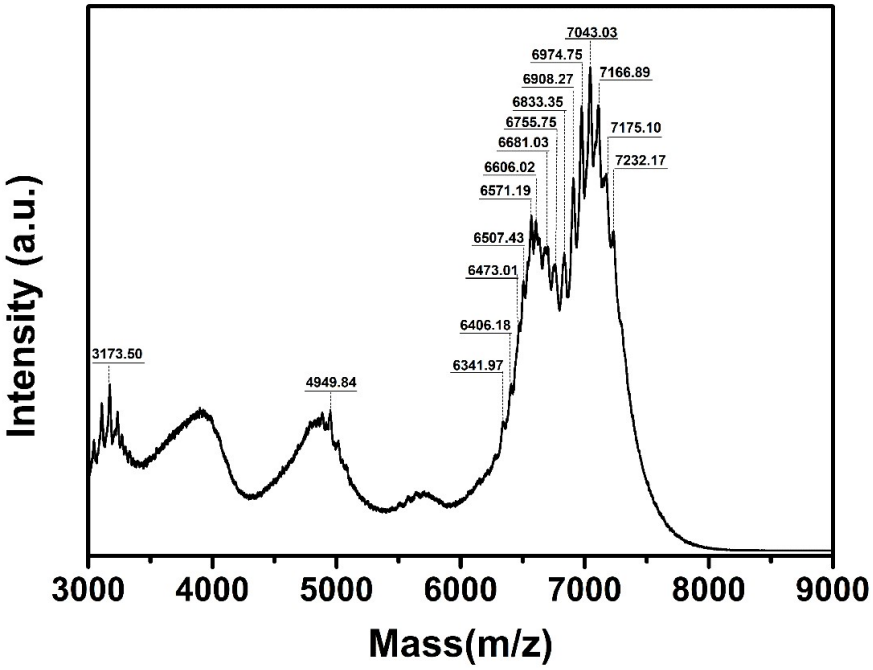

Figure S17. MALDI-TOF MS spectrum of recycled **1**.

Table S4. Photocatalytic oxidative coupling of benzylamine.[a]

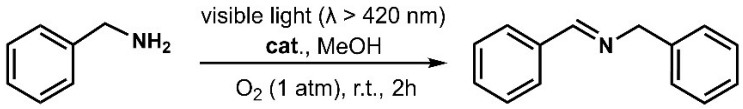

entry	catalyst	light	atmosphere	conversion (%)[b]
1	**1**	+	O_2	> 99
2	PgC_5	+	O_2	< 5
3	CuBr	+	O_2	< 5
4	$CuBr_2$	+	O_2	<5
5	none	+	O_2	< 5
6	**1**	+	N_2	< 5
7	**1**	-	O_2	< 3

[a]Reaction condition: catalyst (10 mg), benzylamine (0.2 mmol), O_2 (1 atm), 2 mL methanol, 300 W xenon lamp with visible light (λ > 420 nm, 100 mW/cm^2), room temperature, 2 hours. [b]Determined based on ^{1}H NMR data.

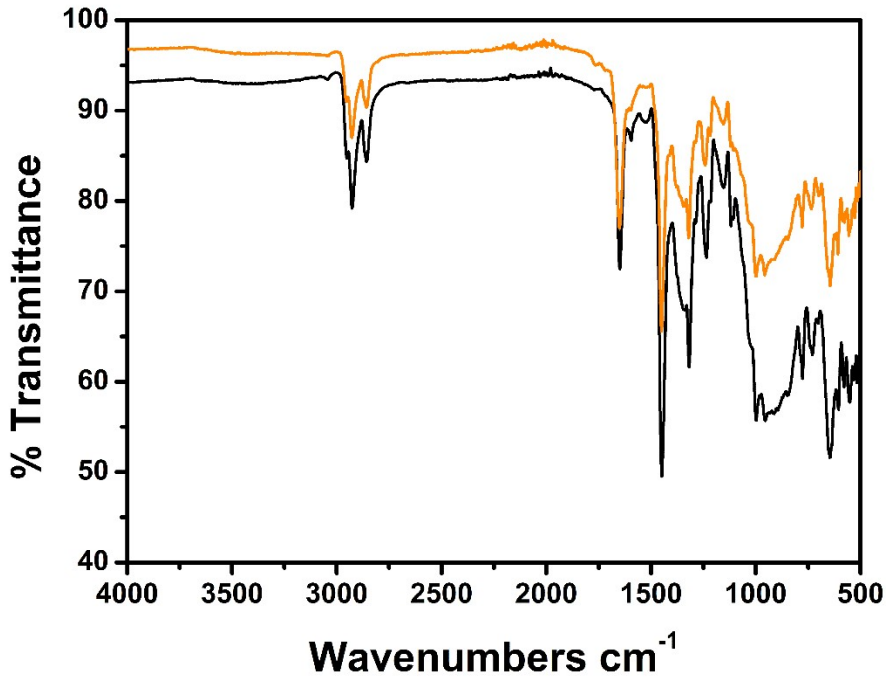

Figure S18. IR spectra of **1** (black line) and recycled **1** (orange line).

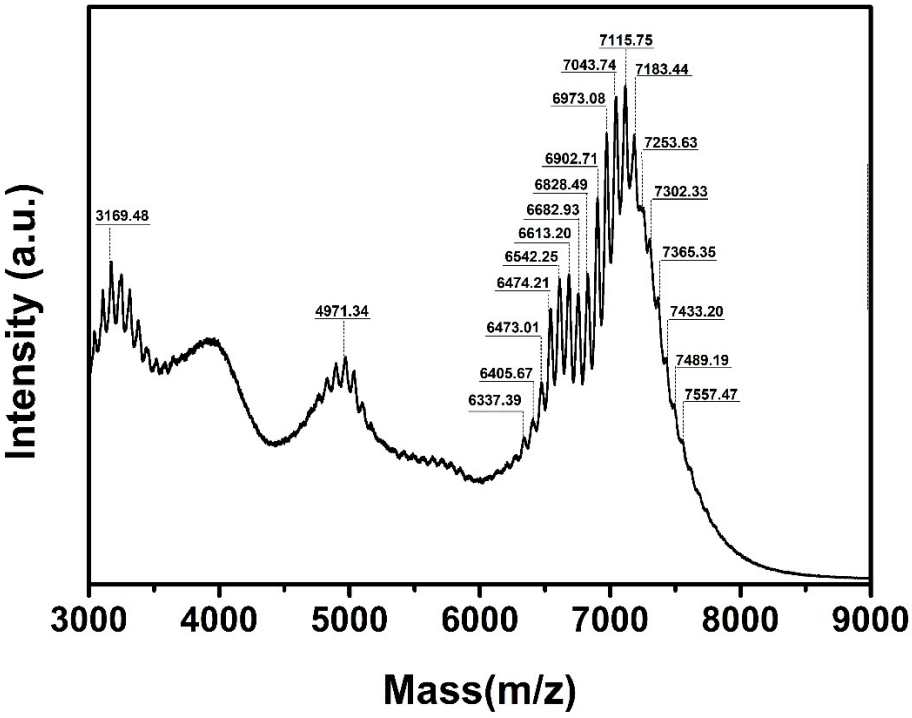

Figure S19. MALDI-TOF MS spectrum of recycled **1**.

Characterization data of products

Phenol

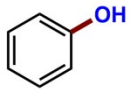

White solid (35.1 mg, 93% yield), EA/PE = 1/10. ^{1}H NMR (400 MHz, *d*-DMSO) δ 9.361 (s, 1H), 7.168 (t, *J* = 8Hz, 2H), 6.783-6.762 (m, 3H). ^{13}C NMR (100 MHz, *d*-DMSO) δ 157.78, 129.83, 119.25, 115.68.

4-methylphenol

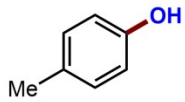

White solid (39.0 mg, 90% yield), EA/PE = 1/10. ^{1}H NMR (400 MHz, $CDCl_3$) δ 7.039-7.025 (m, 2H), 6.729 (dt, *J* = 5.6, 2 Hz, 2H), 2.271 (s, 3H). ^{13}C NMR (100 MHz, $CDCl_3$) δ 153.10, 130.12, 115.15, 20.49.

4-methoxyphenol

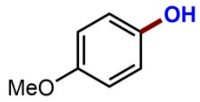

White solid (43.5 mg, 88% yield), EA/PE = 1/5. ^{1}H NMR (400 MHz, $CDCl_3$) δ 6.804-6.750 (m, 4H), 4.654 (m, 1H), 3.761 (s, 3H). ^{13}C NMR (100 MHz, $CDCl_3$) δ 153.54, 149.57, 116.23, 115.07, 55.98.

4-chlorine phenol

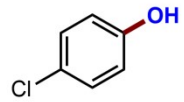

White solid (46.8 mg, 91% yield); EA/PE = 1/10. ^{1}H NMR (400 MHz, $CDCl_3$) δ 7.188 (dt, *J* = 8.8, 3.2 Hz, 2H), 6.761 (dt, *J* = 8.8, 3.6 Hz, 2H), 4.766 (s, 1H). ^{13}C NMR (100 MHz, $CDCl_3$) δ 153.81, 129.64, 125.91, 116.75.

4-Cyanophenol

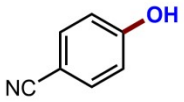

White solid (44.2 mg, 93% yield); EA/PE = 1/5. ^{1}H NMR (400 MHz, $CDCl_3$) δ 7.556 (dt, *J* = 8.8, 2.8 Hz, 2H), 6.911 (dt, *J* = 8.8, 2.8 Hz, 2H), 5.839-5.791 (m, 1H). ^{13}C NMR (100 MHz, $CDCl_3$) δ 160.23, 134.37, 119.27, 116.50, 103.05.

***p*-hydroxy benzaldehyde**

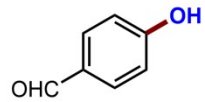

White solid (42.8 mg, 88% yield); EA/PE = 1/5. ^{1}H NMR (400 MHz, $CDCl_3$) δ 9.862 (1H), 7.818 (dt, J = 8.4, 2.8 Hz, 2H), 6.970 (dt, J = 8.4, 2.4 Hz, 2H), 6.084 (s, 1H). ^{13}C NMR (100 MHz, $CDCl_3$) δ 191.23, 161.48, 132.54, 129.94, 116.02.

_p_-hydroxybenzoic acid

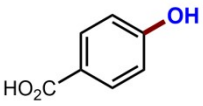

White solid (50.9 mg, 92% yield); EA/PE = 1/5. ^{1}H NMR (400 MHz, *d*-DMSO) δ 12.412 (s, 1H), 10.202 (s, 1H), 7.755 (dt, J = 8.8, 2.8 Hz, 2H), 6.788 (dt, J = 8.8, 2.8 Hz, 2H). ^{13}C NMR (100 MHz, *d*-DMSO) δ 167.62, 162.06, 131.99, 121.80, 115.58.

4-phenylphenol

White solid (60.5 mg, 89% yield); EA/PE = 1/10. ^{1}H NMR (400 MHz, $CDCl_3$) δ 7.537 (d, J = 7.2 Hz, 2H), 7.479 (d, J = 8.8 Hz, 2H), 7.412 (t, J = 7.6 Hz, 2H), 7.302 (t, J = 7.2 Hz, 1H), 6.904 (d, J = 8.8 Hz, 2H), 4.849 (s, 1H). ^{13}C NMR (100 MHz, $CDCl_3$) δ 155.02, 140.75, 134.10, 128.75, 128.42, 126.74, 115.66.

hydroquinone

White solid (36.9 mg, 84% yield); EA/PE = 1/5. ^{1}H NMR (400 MHz, d-DMSO) δ 8.601 (s, 4H), 6.522 (s, 2H). ^{13}C NMR (100 MHz, d-DMSO) δ 150.19, 116.10.

4-hydroxypyridine

White solid (33.4 mg, 88% yield); EA/PE = 1/2. ^{1}H NMR (400 MHz, *d*-DMSO) δ 11.343 (brs, 1H), 7.677 (d, J = 6.8 Hz, 2H), 6.143 (d, J = 6.8 Hz, 2H). ^{13}C NMR (100 MHz, *d*-DMSO) δ 140.24, 116.60.

azobenzene

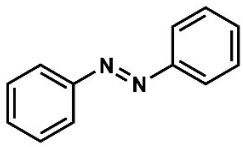

Orange solid (18.0 mg, 99% yield). ^{1}H NMR (400 MHz, $CDCl_3$) δ 7.968-7.950 (m, 4H), 7.576-7.490 (m, 6H). ^{13}C NMR (100 MHz, $CDCl_3$) δ 152.67, 131.01, 129.11, 122.87.

N-benzylidenebenzylamine

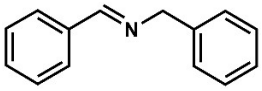

Colorless oil (39.0 mg, 99.9% yield). ^{1}H NMR (400 MHz, d-DMSO) δ 8.509 (s, 1H), 7.801-7.778 (m, 2H), 7.474-7.434 (m, 3H), 7.372-7.239 (m, 5H), 4.775 (s, 2H). ^{13}C NMR (100 MHz, d-DMSO) δ 162.25, 140.07, 136.50, 131.24, 129.16, 128.83, 128.44, 128.38, 127.26, 64.44.

Reference

[1] Apex3, AXScale, and SAINT, version 2017.3-0, Bruker AXS, Inc., Madison, WI, **2017**.

[2] Sheldrick, G. M. SHELXT-Integrated space-group and crystal-structure determination. *Acta Cryst. Sect. A: Found. Adv.* **2015**, 71, 3-8.

[3] Sheldrick, G. M. Crystal structure refinement with SHELXL. *Acta Cryst. Sect. C. Struct. Chem*. **2015**, 71, 3-8.

[4] Thorn, A.; Dittrich, B.; Sheldrick, G. M. Enhanced rigid bond restraints. *Acta Cryst. Sect. A. Found. Adv*. **2012**, 68, 448-451.

[5] Gibb, B. C., Chapman, R.G., Sherman, J. C. Synthesis of hydroxyl-footed cavitands. *J. Org. Chem*. **1996**, 61, 1505-1509.

[6] Brown I., Altermatt, D. Bond-valence parameters obtained from a systematic analysis of the Inorganic Crystal Structure Database. *Acta Cryst. B*, **1985**, 41, 244-247.

^{1}H NMR and ^{13}C NMR spectra

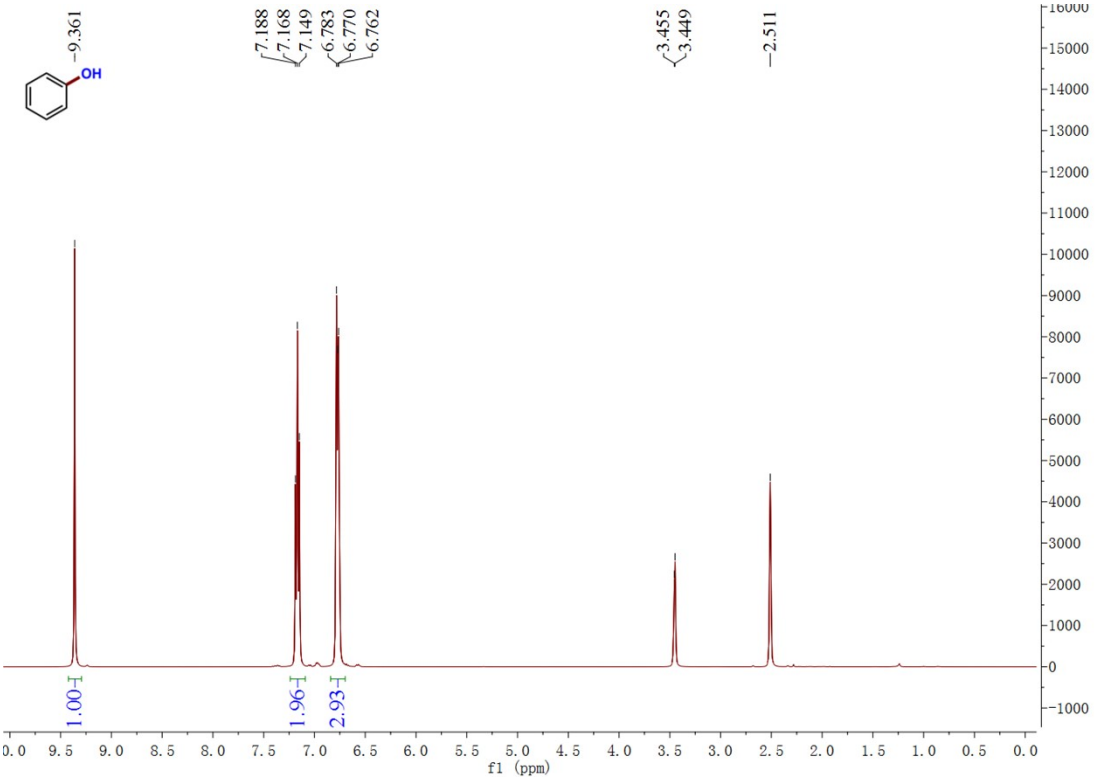

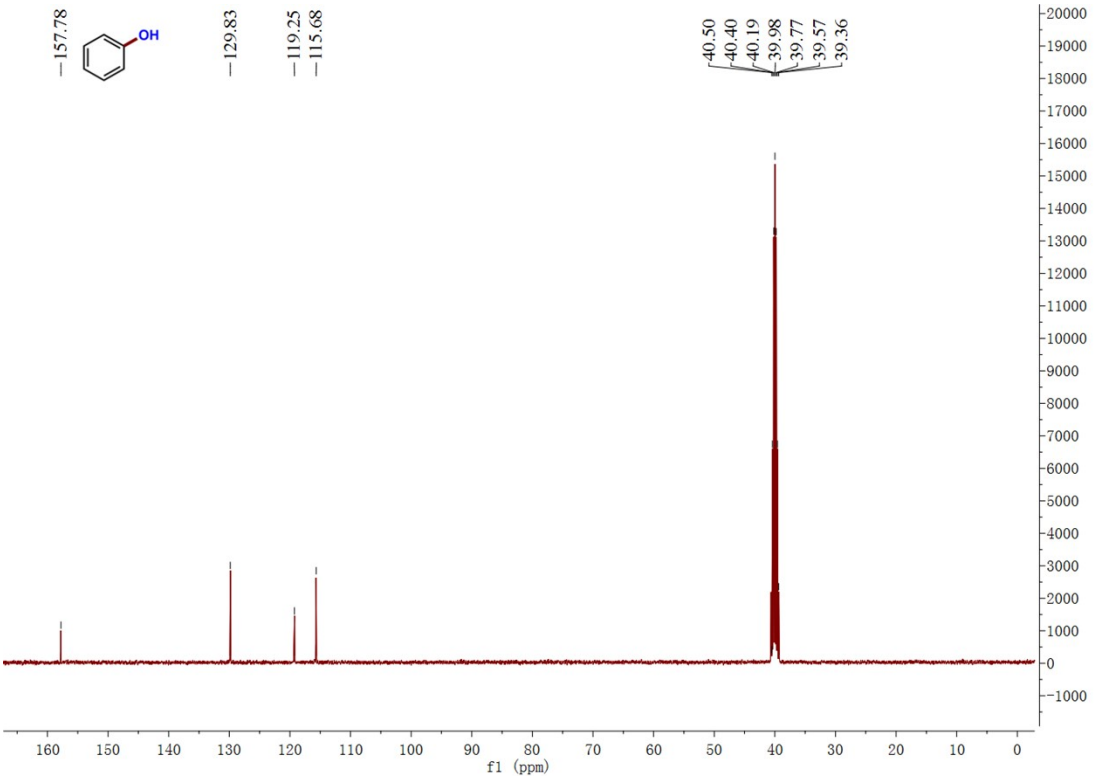

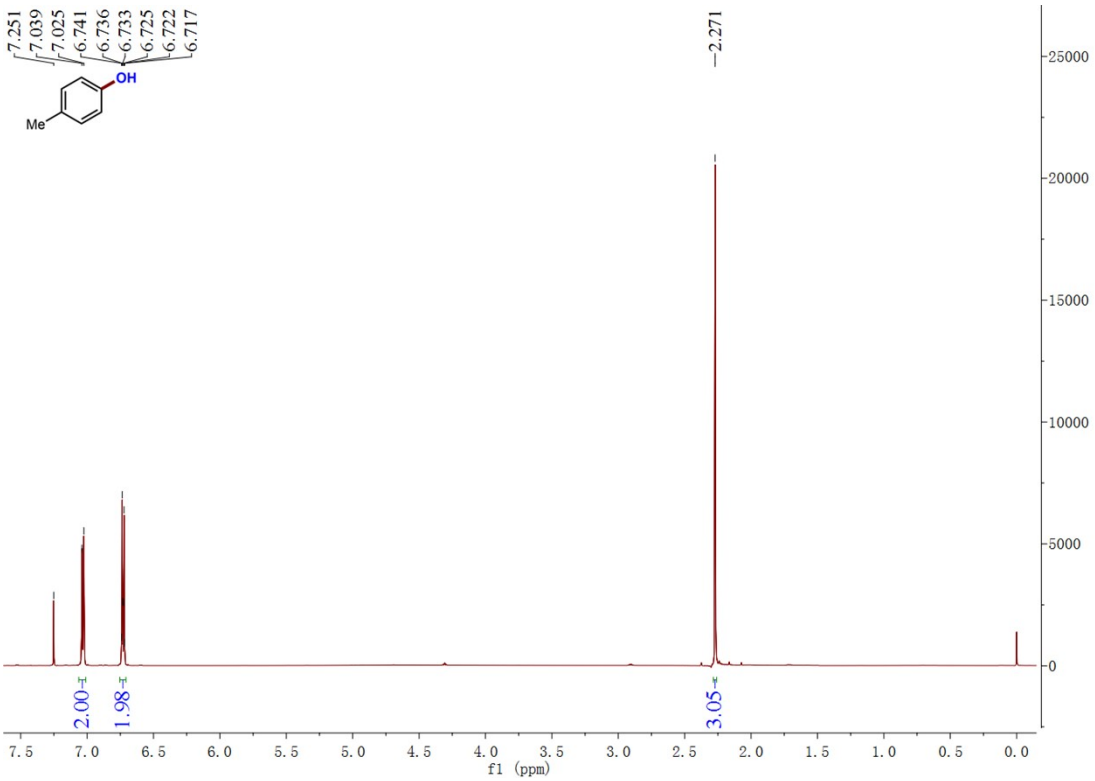
7.251
7.039
7.025
6.741
6.736
6.733
6.725
6.722
6.717
OH
Me
2.271
2.00
1.98
3.05
f1 (ppm)

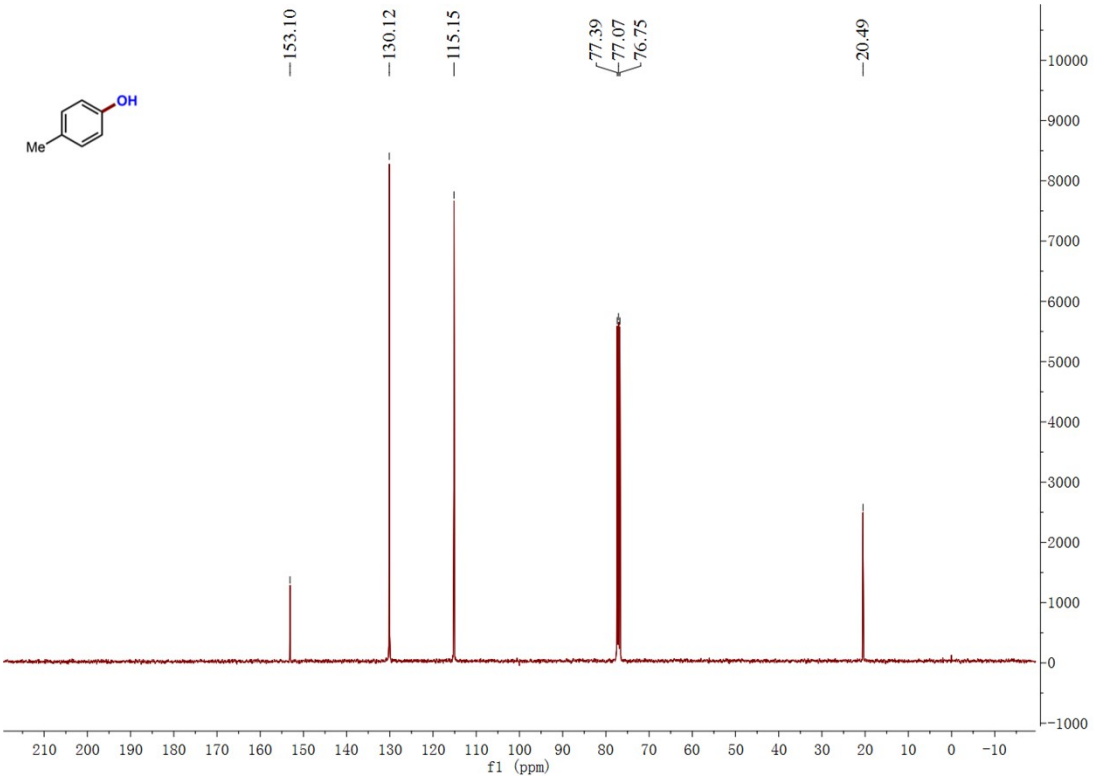
153.10
130.12
115.15
77.39
77.07
76.75
20.49
OH
Me
f1 (ppm)

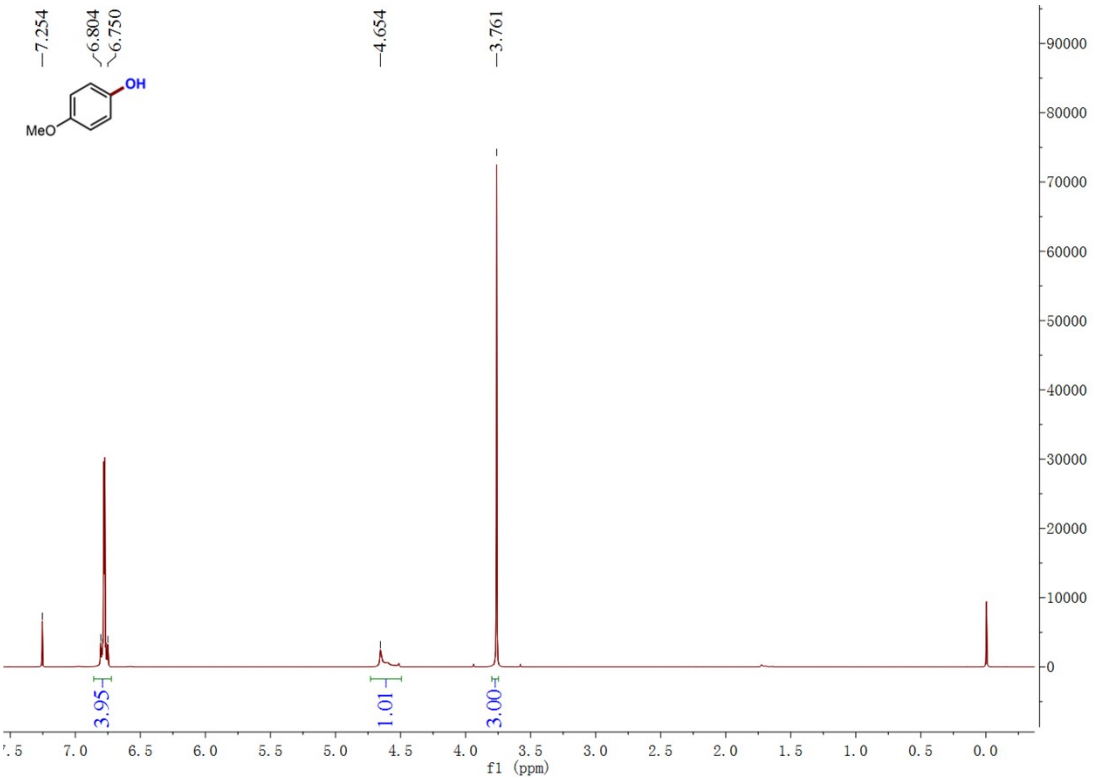
7.254
6.804
6.750
4.654
3.761
OH
MeO
3.95
1.01
3.00
f1 (ppm)

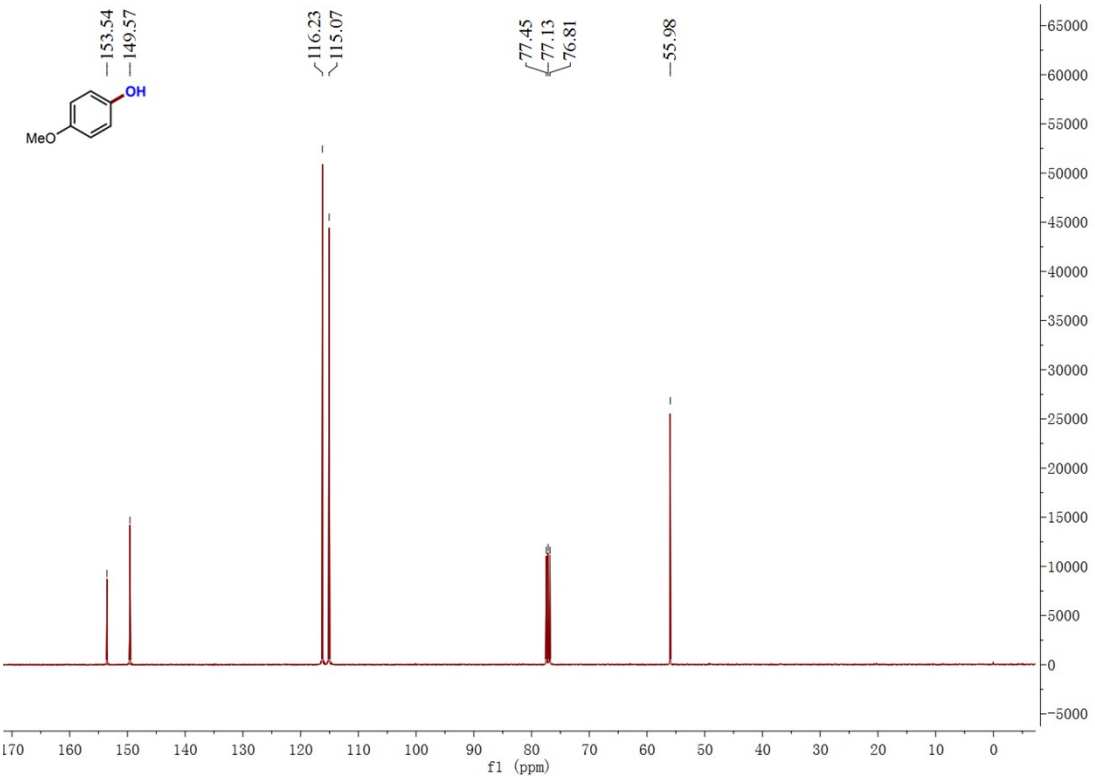
153.54
149.57
116.23
115.07
77.45
77.13
76.81
55.98
OH
MeO
f1 (ppm)

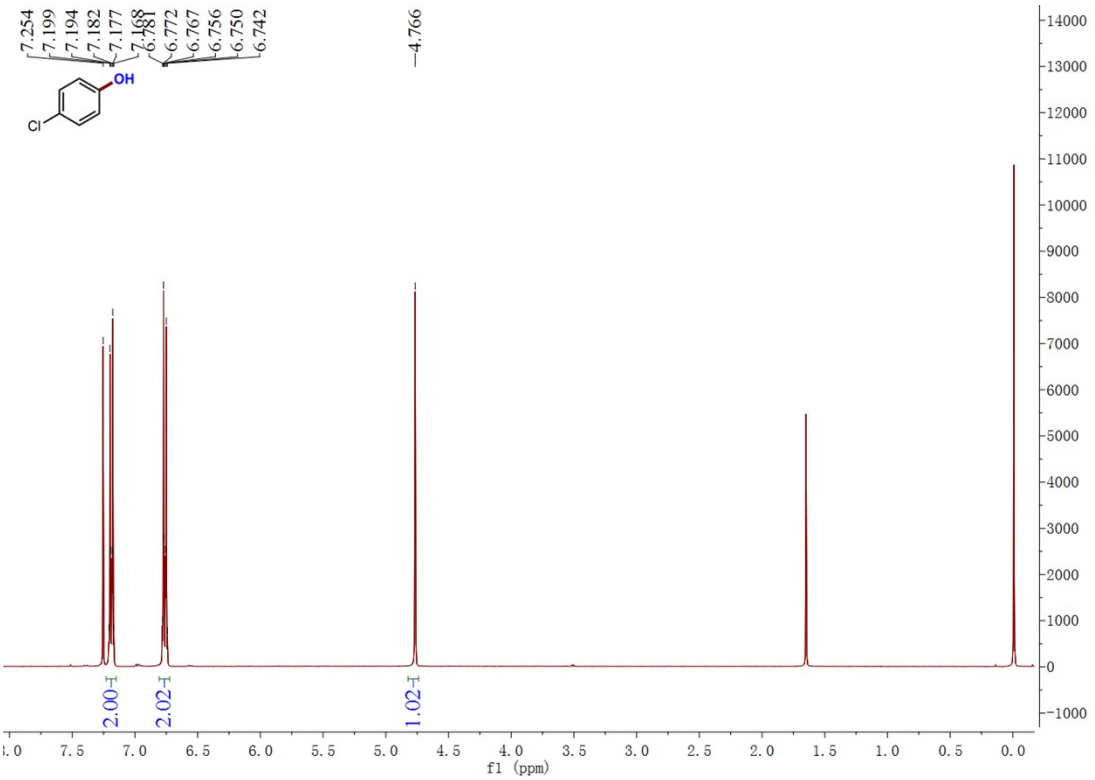
7.254
7.199
7.194
7.182
7.177
7.168
6.781
6.772
6.767
6.756
6.750
6.742
4.766
OH
Cl
2.00
2.02
1.02
f1 (ppm)

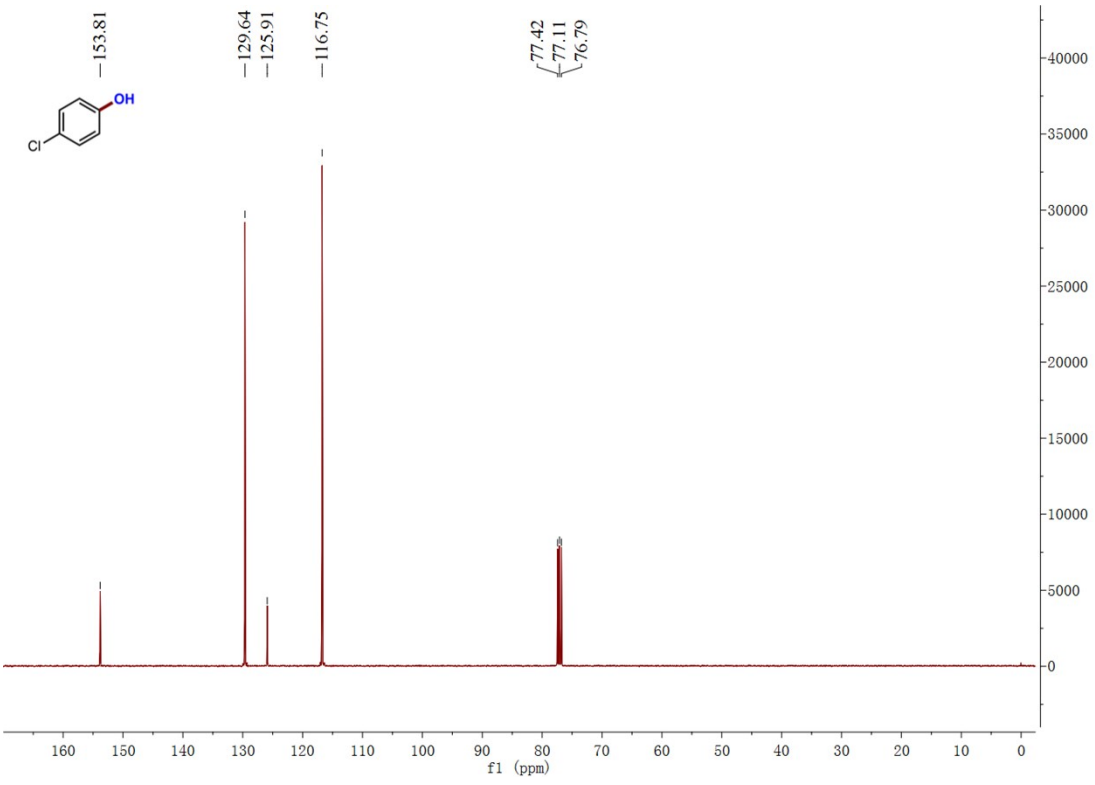
153.81
129.64
125.91
116.75
77.42
77.11
76.79
OH
Cl
f1 (ppm)

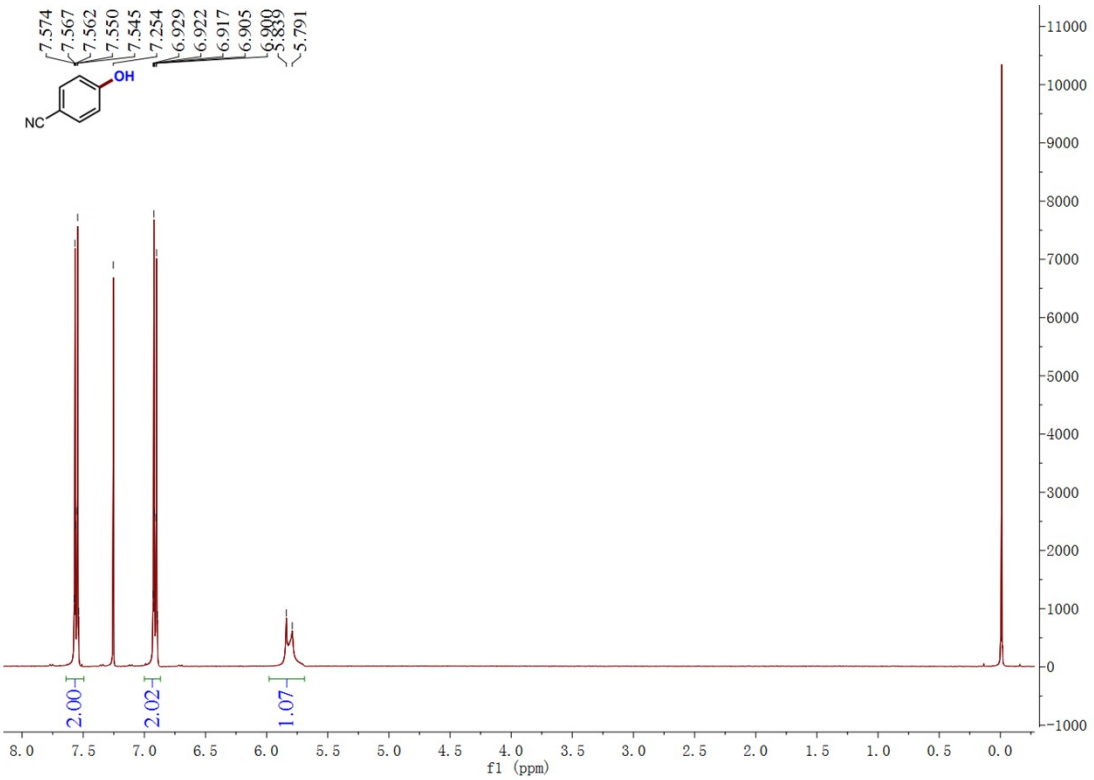
7.574
7.567
7.562
7.550
7.545
7.254
6.929
6.922
6.917
6.905
6.900
5.839
5.791
OH
NC
2.00
2.02
1.07
f1 (ppm)

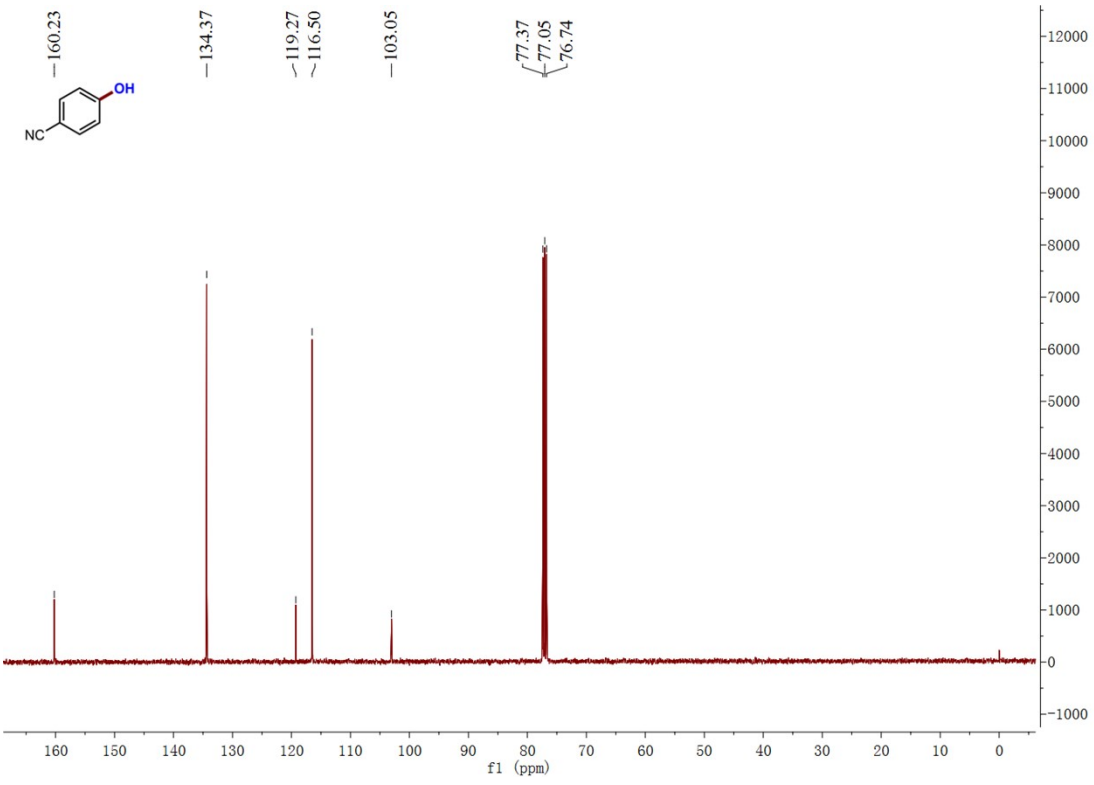
160.23
134.37
119.27
116.50
103.05
77.37
77.05
76.74
OH
NC
f1 (ppm)

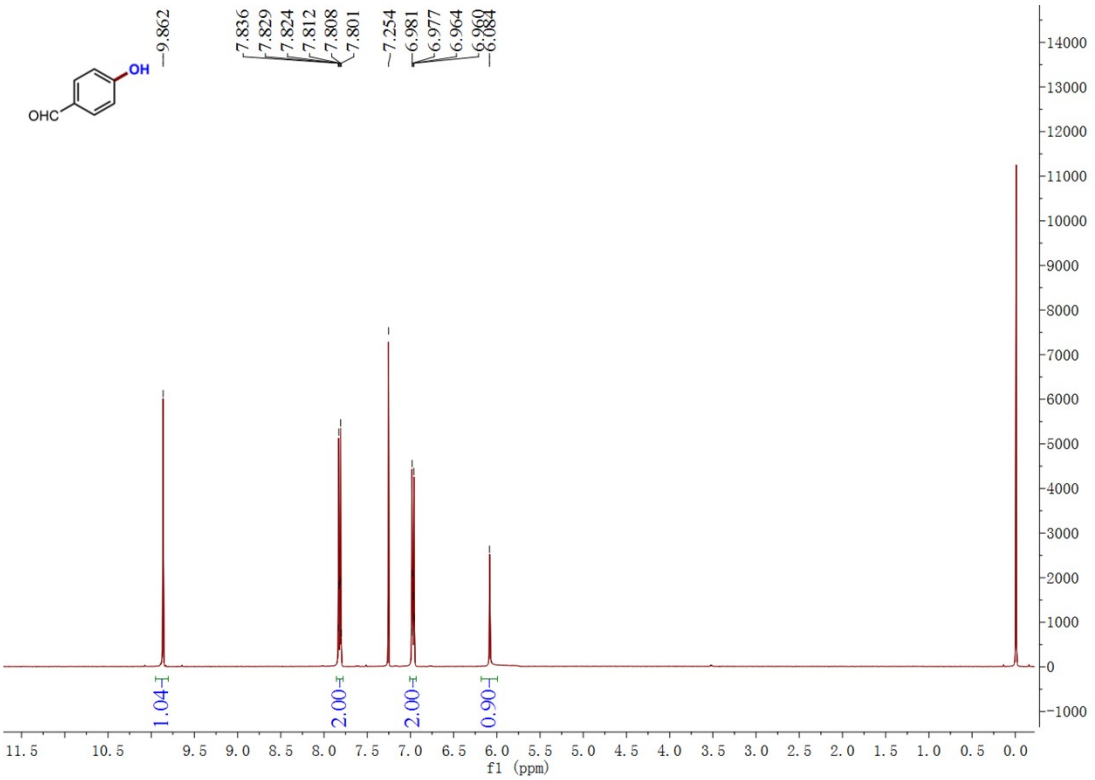
9.862
7.836
7.829
7.824
7.812
7.808
7.801
7.254
6.981
6.977
6.964
6.960
6.084
OH
OHC
1.04
2.00
2.00
0.90
f1 (ppm)

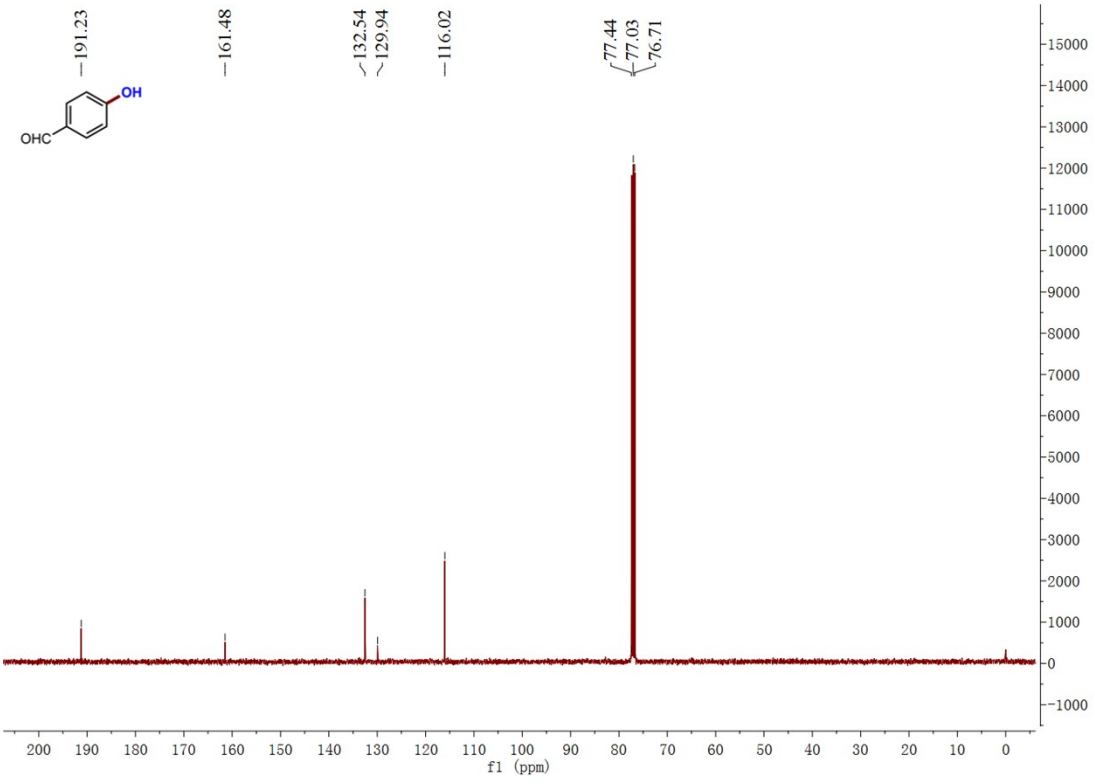
191.23
161.48
132.54
129.94
116.02
77.44
77.03
76.71
OH
OHC
f1 (ppm)

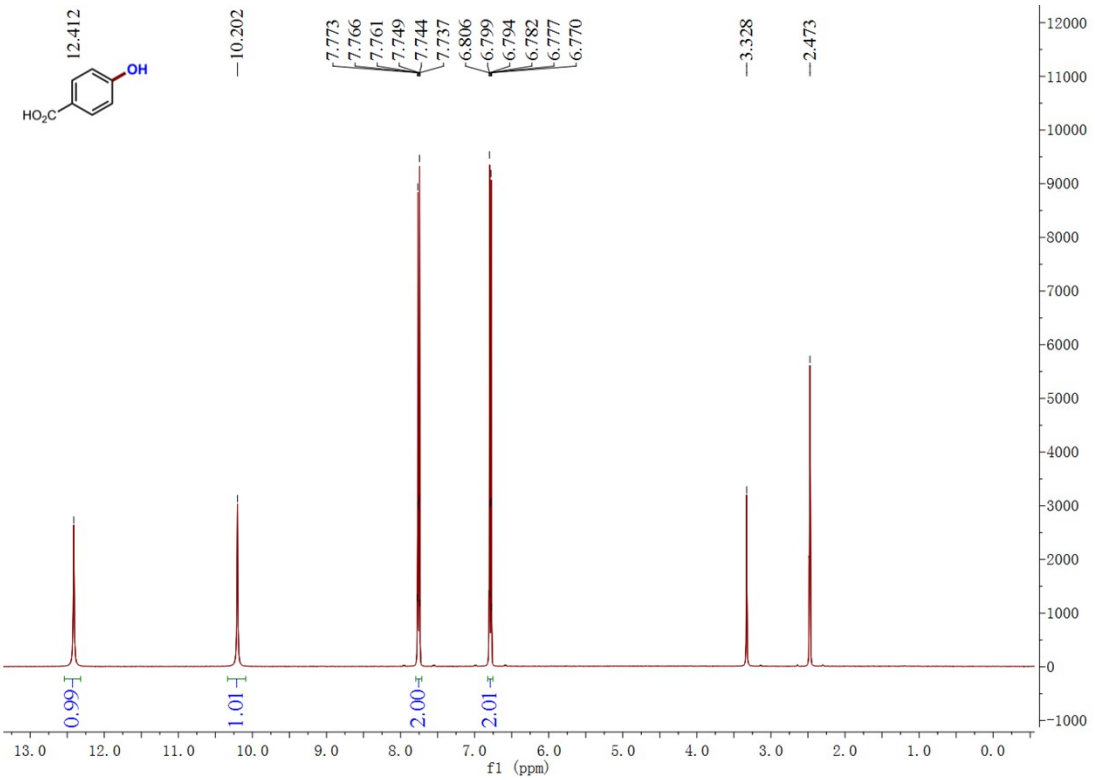
12.412
10.202
7.773
7.766
7.761
7.749
7.744
7.737
6.806
6.799
6.794
6.782
6.777
6.770
3.328
2.473
OH
HO2C
0.99
1.01
2.00
2.01
f1 (ppm)

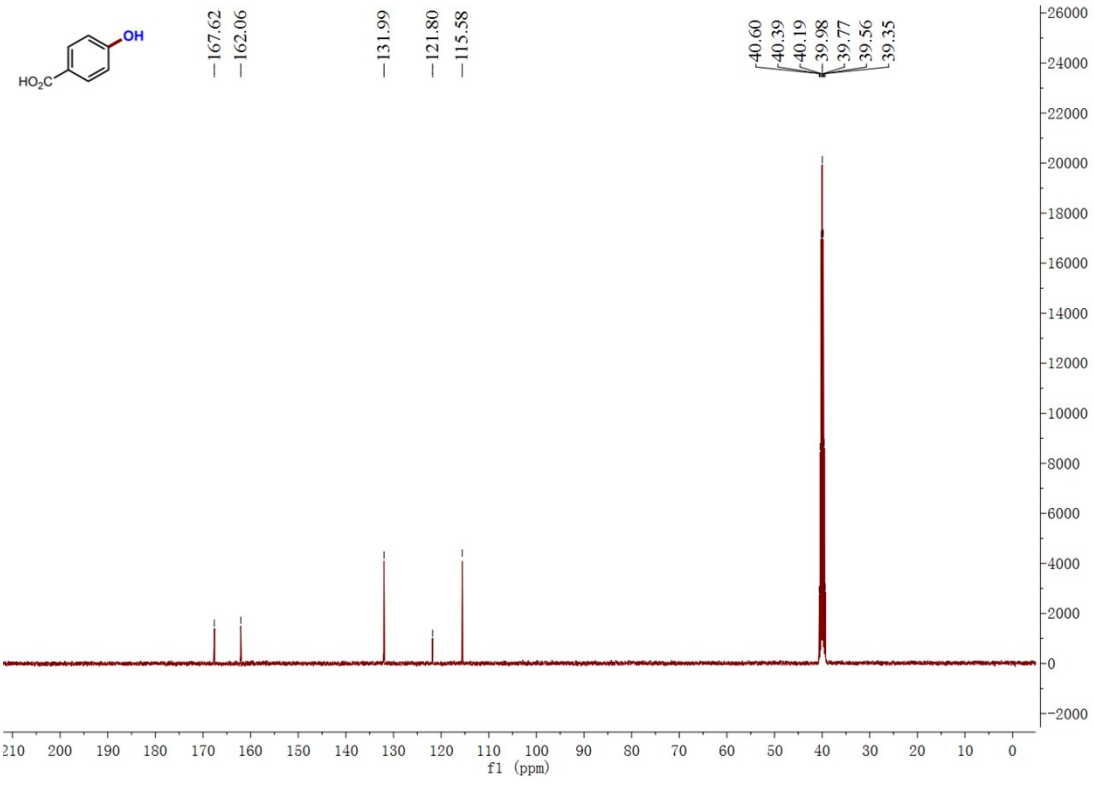
167.62
162.06
131.99
121.80
115.58
40.60
40.39
40.19
39.98
39.77
39.56
39.35
OH
HO2C
f1 (ppm)

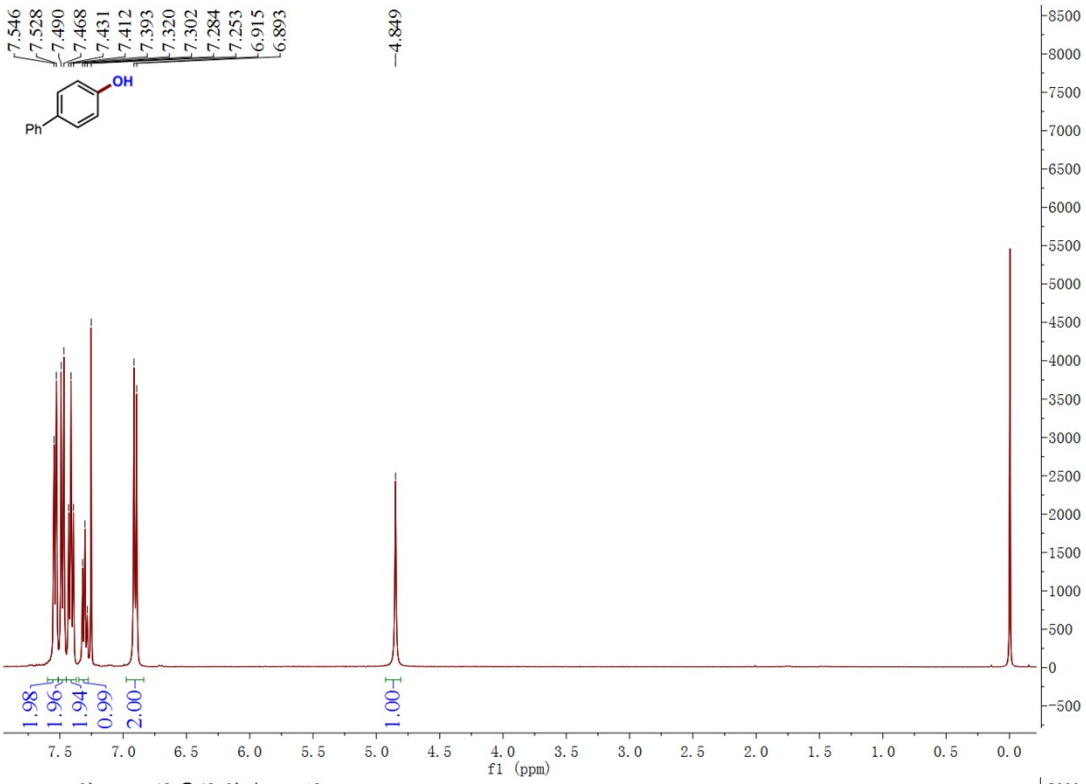
7.546
7.528
7.490
7.468
7.431
7.412
7.393
7.320
7.302
7.284
7.253
6.915
6.893
4.849
OH
Ph
1.98
1.96
1.94
0.99
2.00
1.00
f1 (ppm)

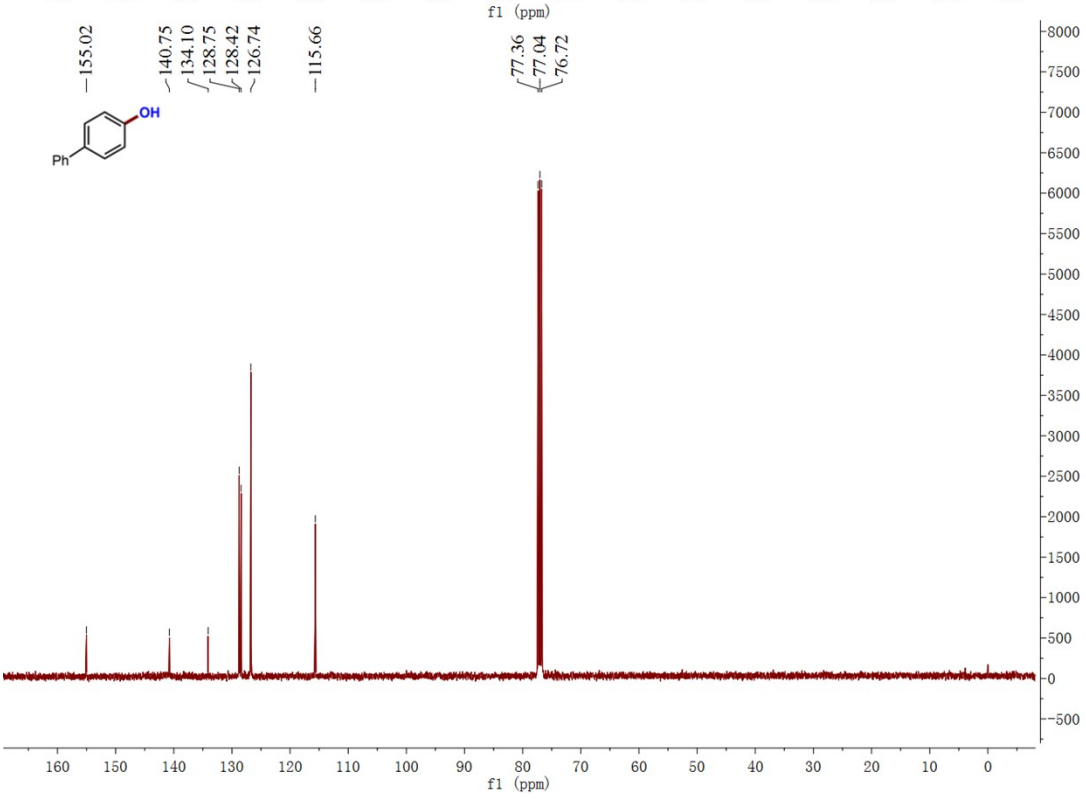
155.02
140.75
134.10
128.75
128.42
126.74
115.66
77.36
77.04
76.72
OH
Ph
f1 (ppm)

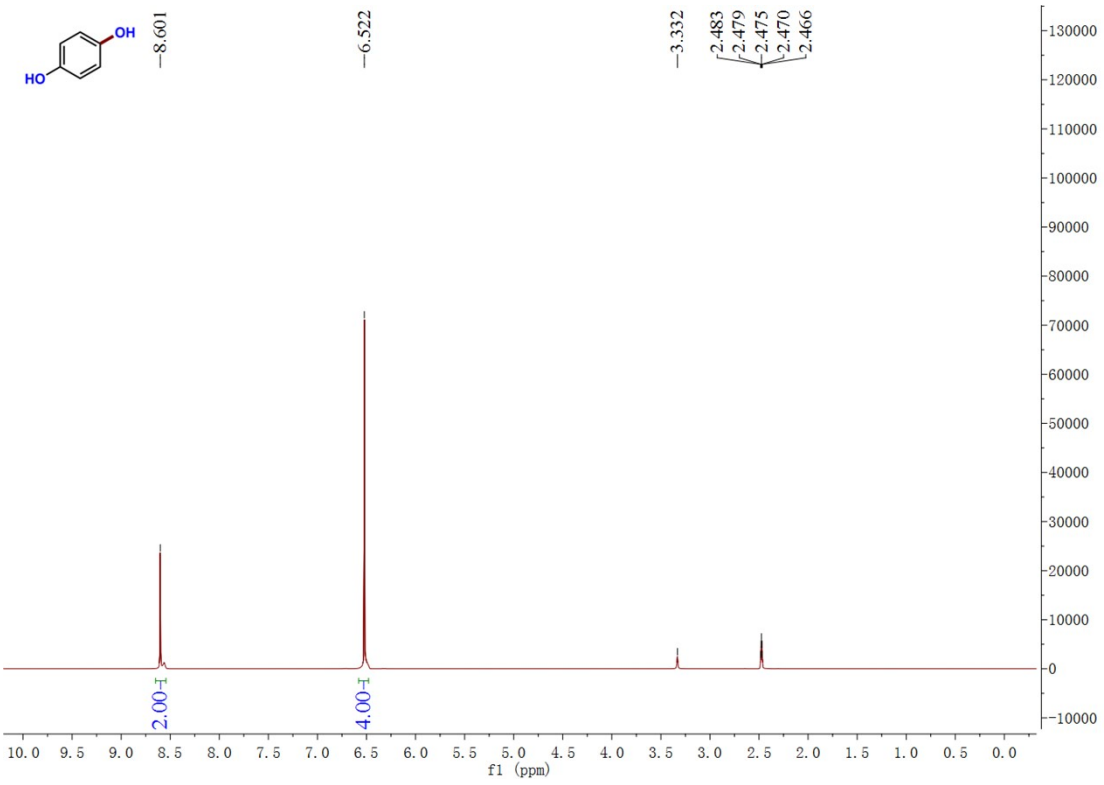
OH
HO
8.601
6.522
3.332
2.483
2.479
2.475
2.470
2.466
2.00
4.00
f1 (ppm)

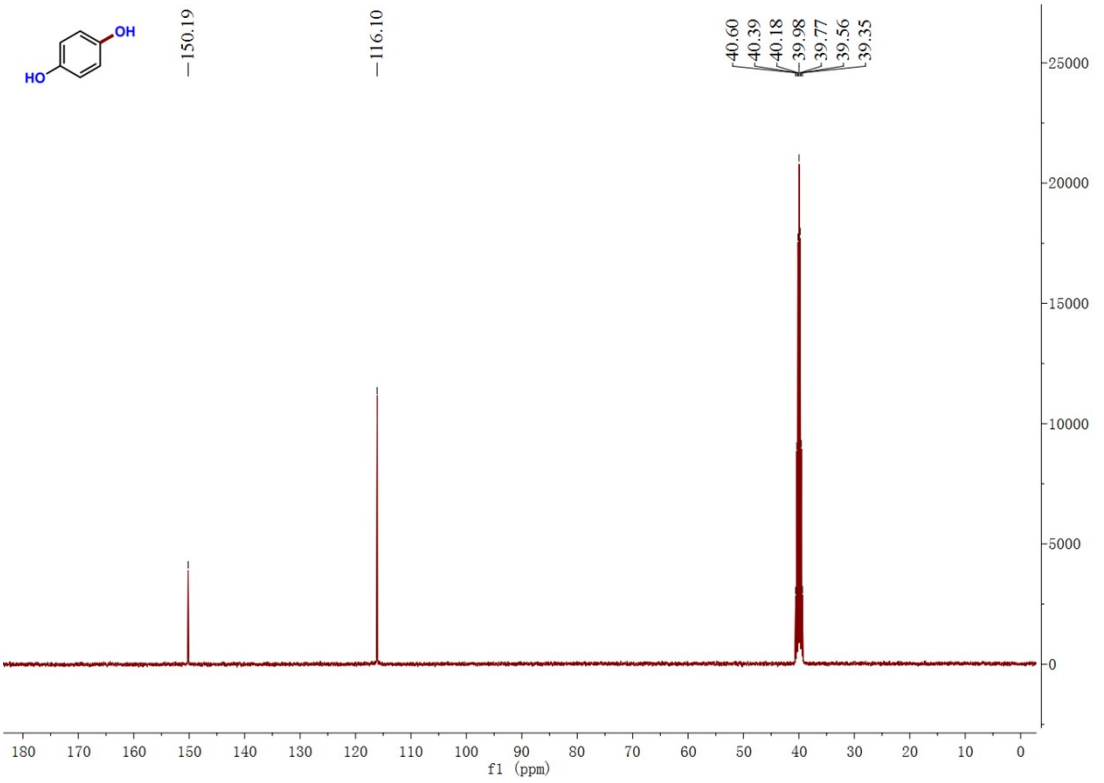
OH
HO
150.19
116.10
40.60
40.39
40.18
39.98
39.77
39.56
39.35
f1 (ppm)

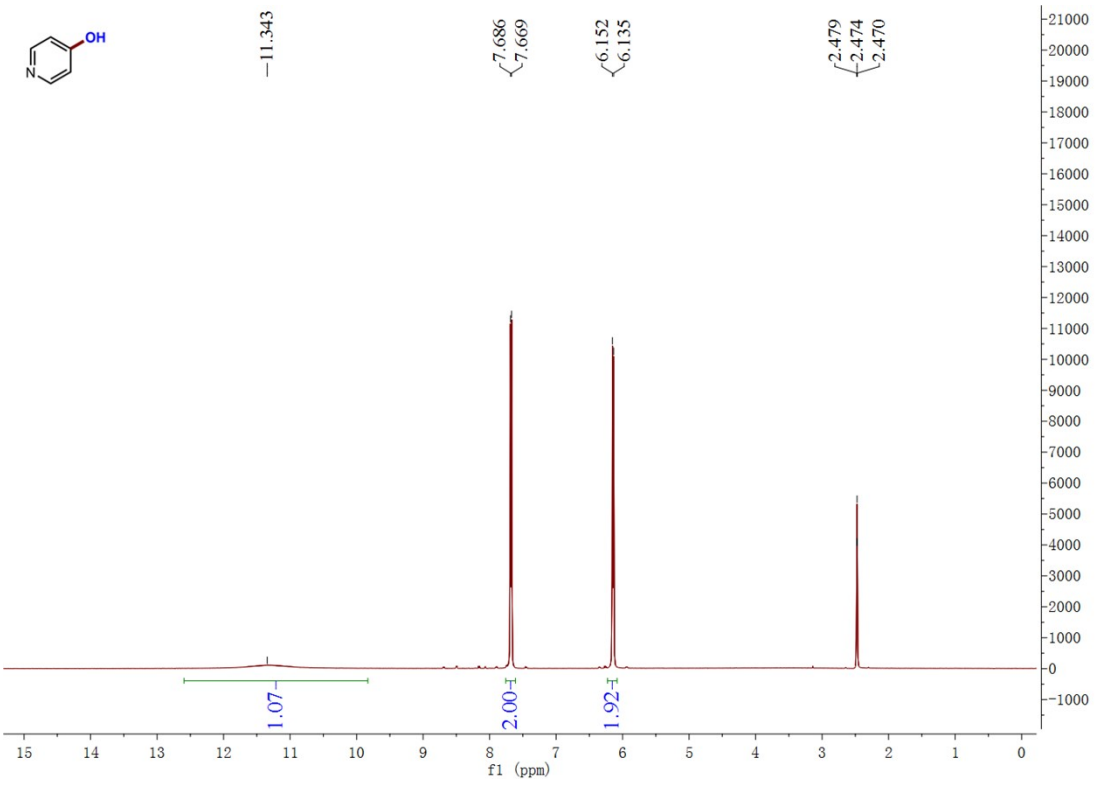
OH
N
11.343
7.686
7.669
6.152
6.135
2.479
2.474
2.470
1.07
2.00
1.92
f1 (ppm)

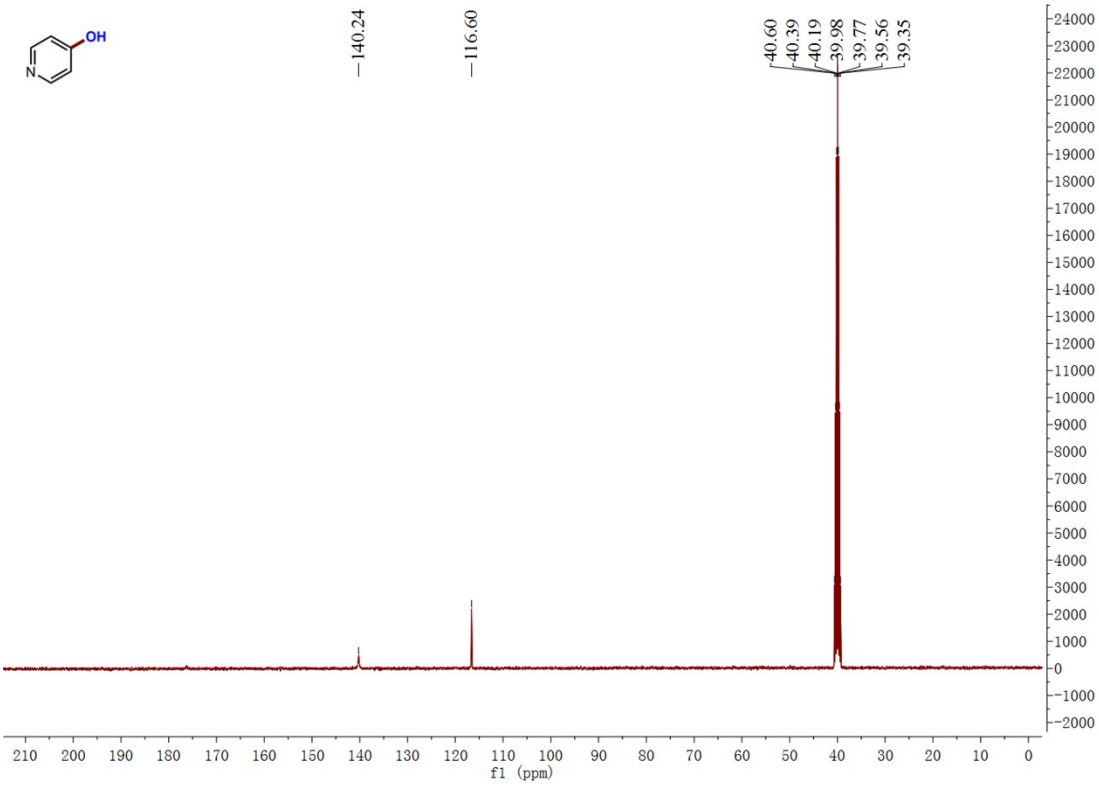
OH
N
140.24
116.60
40.60
40.39
40.19
39.98
39.77
39.56
39.35
f1 (ppm)

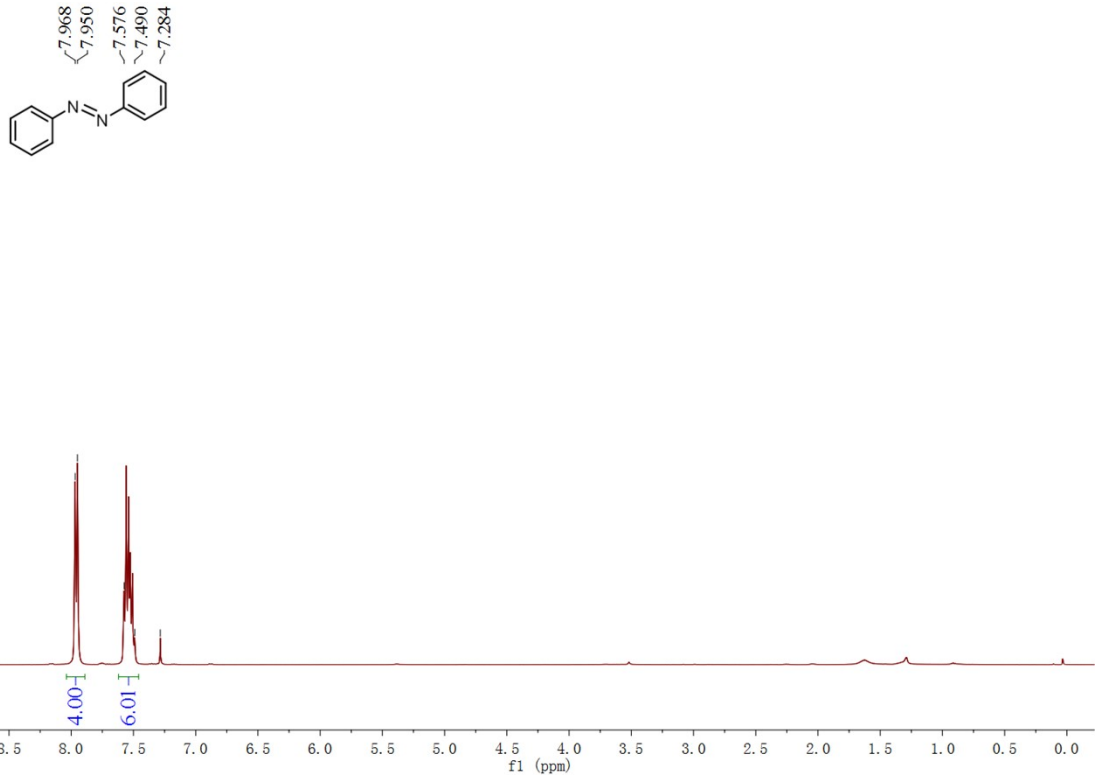
7.968
7.950
7.576
7.490
7.284
4.00
6.01
f1 (ppm)

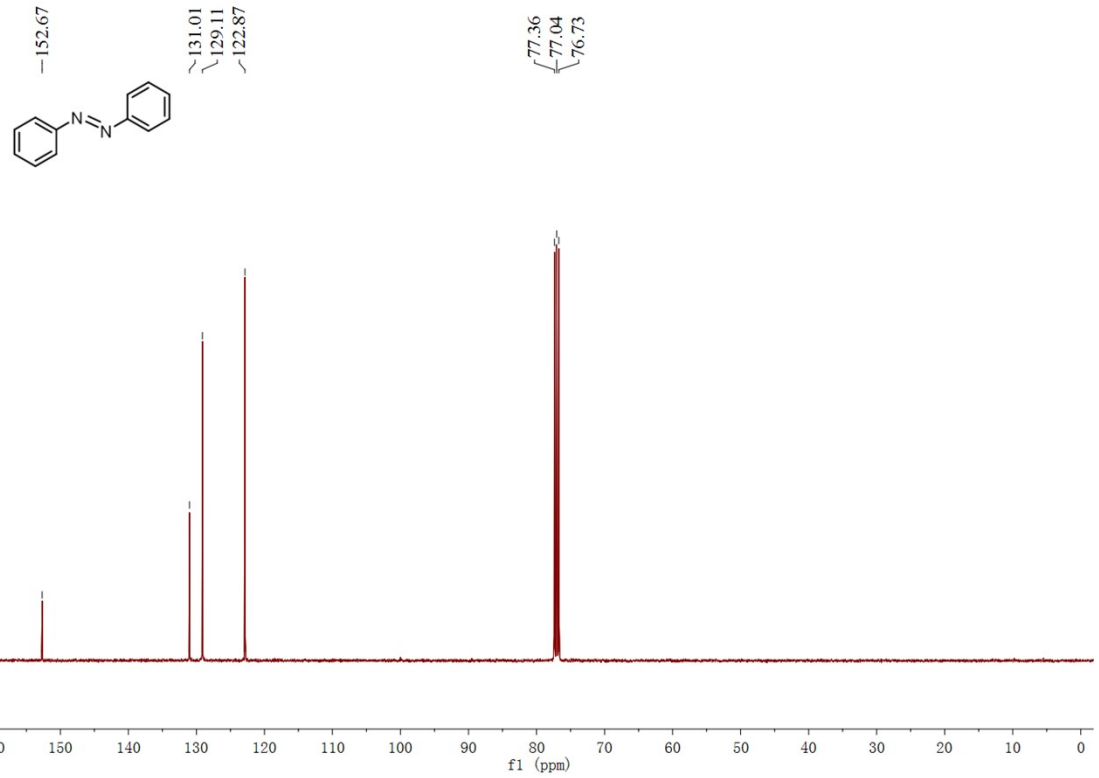
152.67
131.01
129.11
122.87
77.36
77.04
76.73
f1 (ppm)

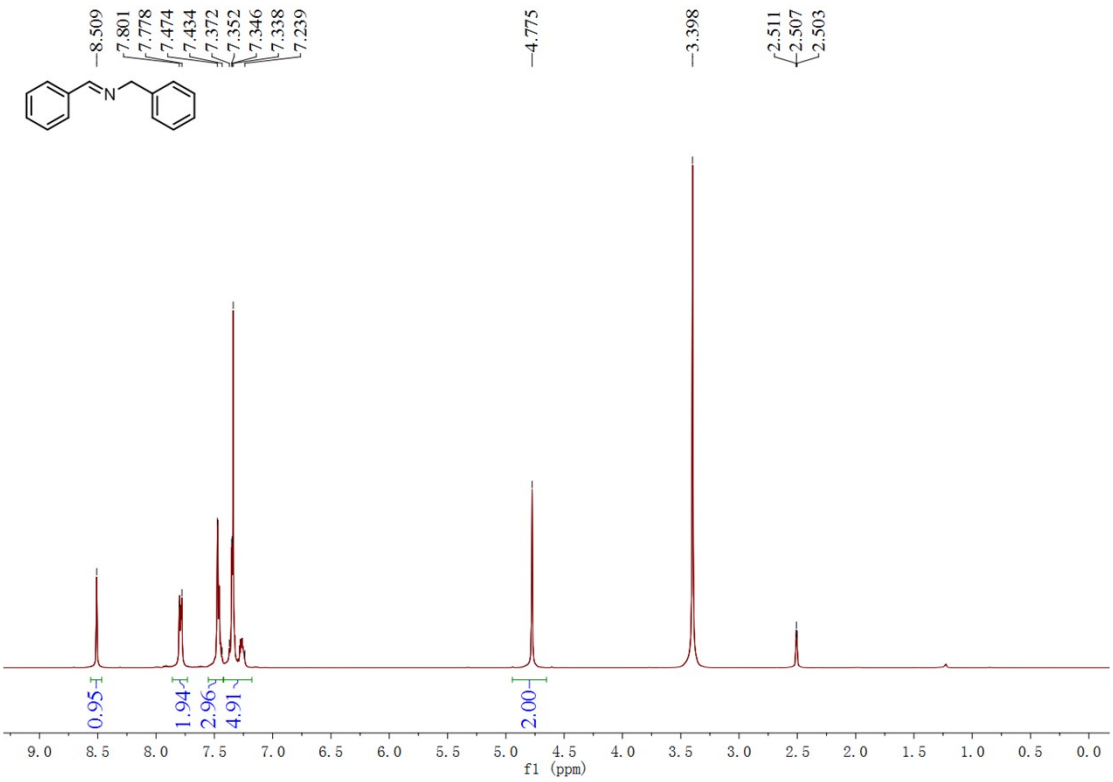
8.509
7.801
7.778
7.474
7.434
7.372
7.352
7.346
7.338
7.239
4.775
3.398
2.511
2.507
2.503
0.95
1.94
2.96
4.91
2.00
f1 (ppm)

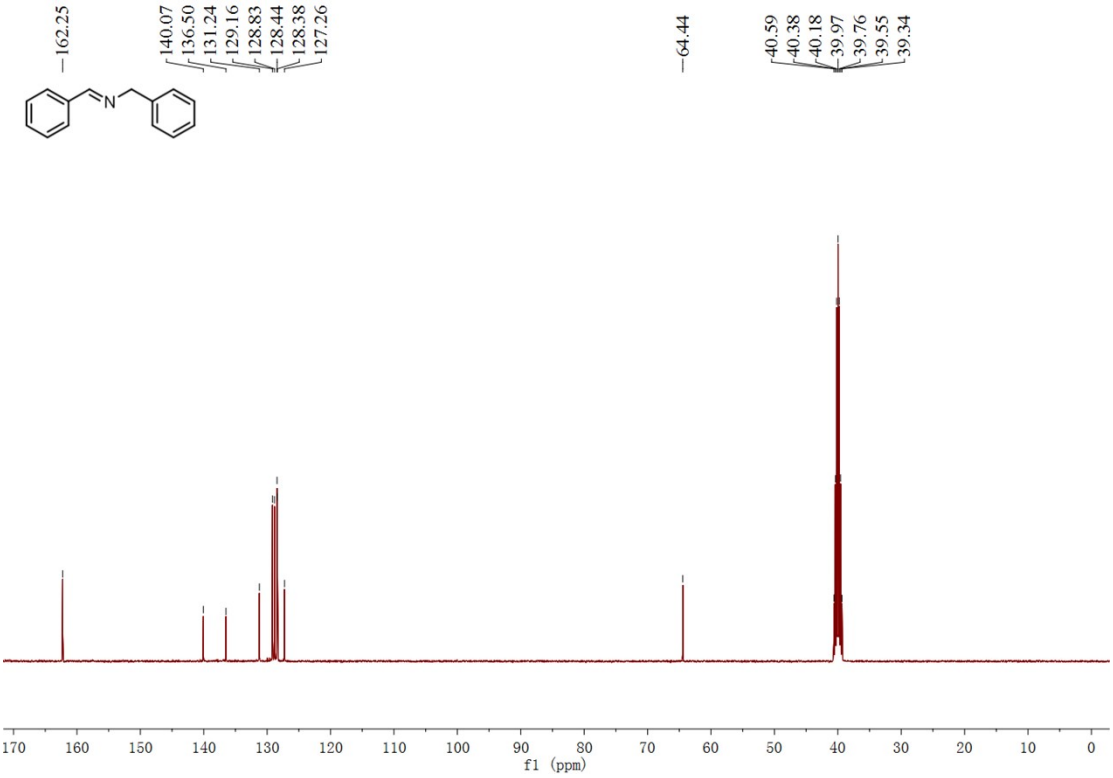
162.25
140.07
136.50
131.24
129.16
128.83
128.44
128.38
127.26
64.44
40.59
40.38
40.18
39.97
39.76
39.55
39.34
f1 (ppm)